Imaging in random media

Chrysoula Tsogka

tsogka@math.uchicago.edu

University of Chicago

In Collaboration with:

Liliana Borcea (Rice University)

George Papanicolaou (Stanford University)

Passive Array Imaging in Clutter

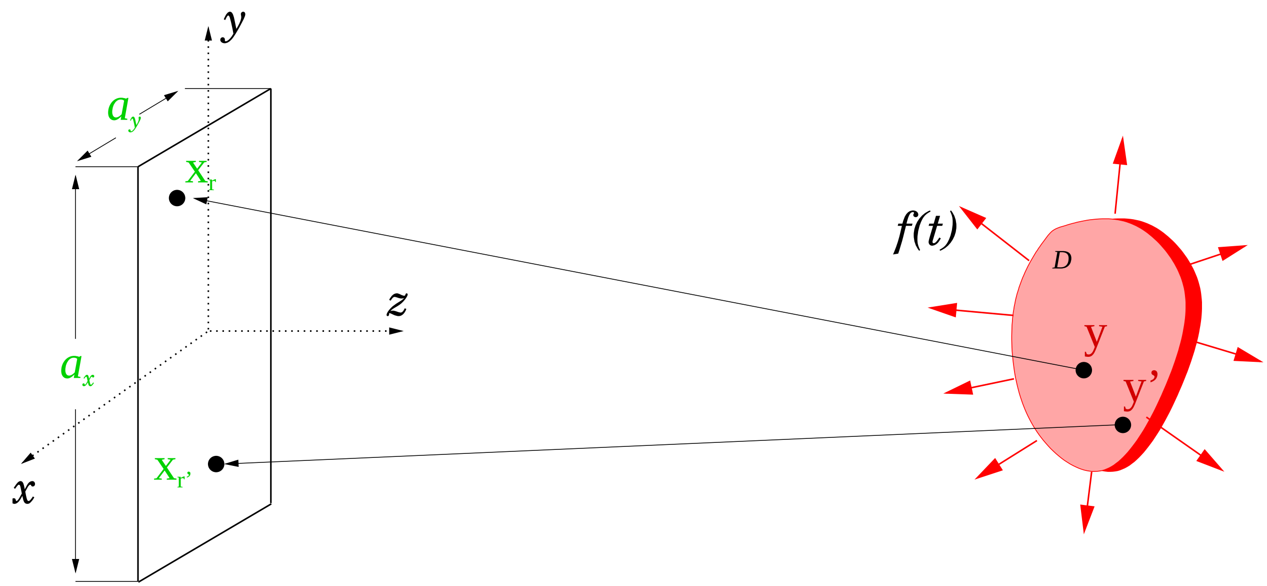

- Array data: $P(\mathbf{x}_r, t)$ for $(\mathbf{x}_r, t)$ a set of receiver locations in $\mathbb{R}^2$ and time in $\mathbb{R}_+$.
- Object: continuous distribution of sources in $\mathcal{D}$ with intensity $\varrho(\mathbf{y})$.

Passive Array Imaging in Clutter

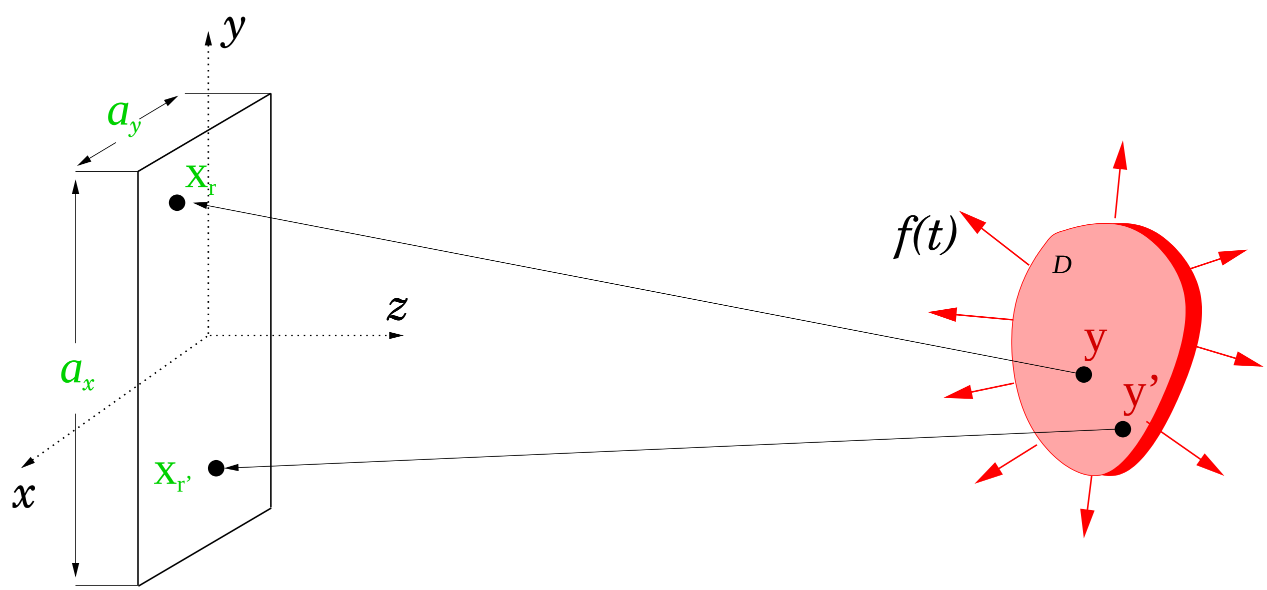

- Objective: recover $\mathcal{D}$ from $P(\mathbf{x}_r, t)$ when the background medium is cluttered.

Active Array Imaging in Clutter

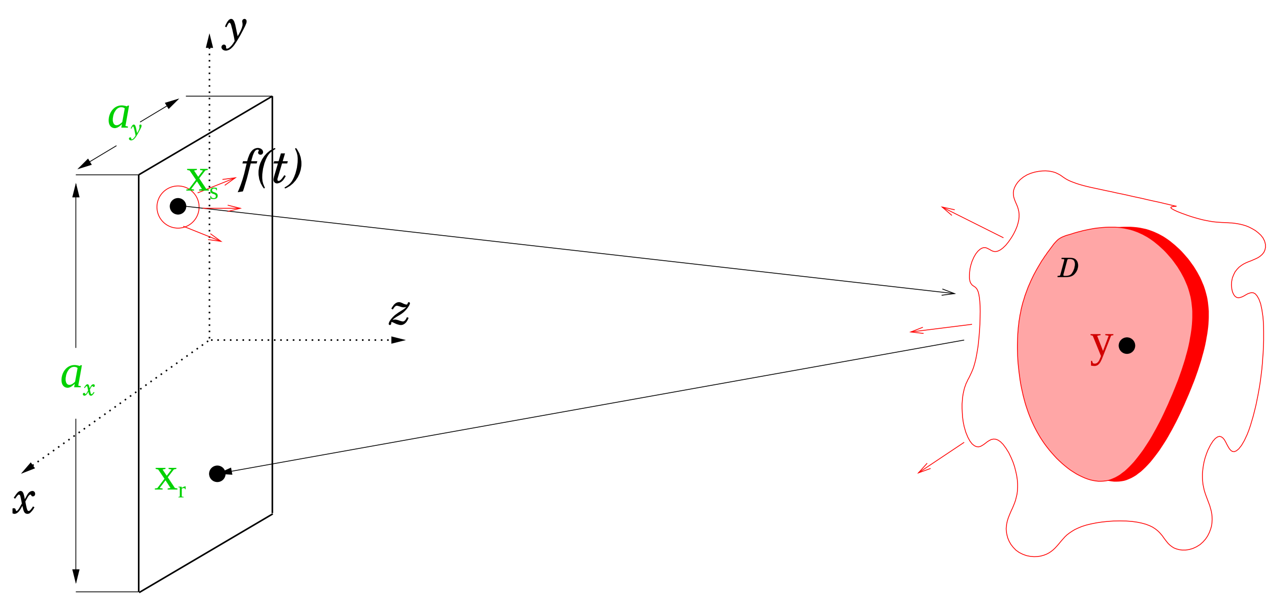

- Array data: $P(\mathbf{x}_s, \mathbf{x}_r, t)$ for $(\mathbf{x}_s, \mathbf{x}_r, t)$ a set of source and receiver locations in $\mathbb{R}^2$ and time in $\mathbb{R}_+$.
- Object: scatterrer with support in $\mathcal{D}$ and reflectivity $\varrho(\mathbf{y})$.

Active Array Imaging in Clutter

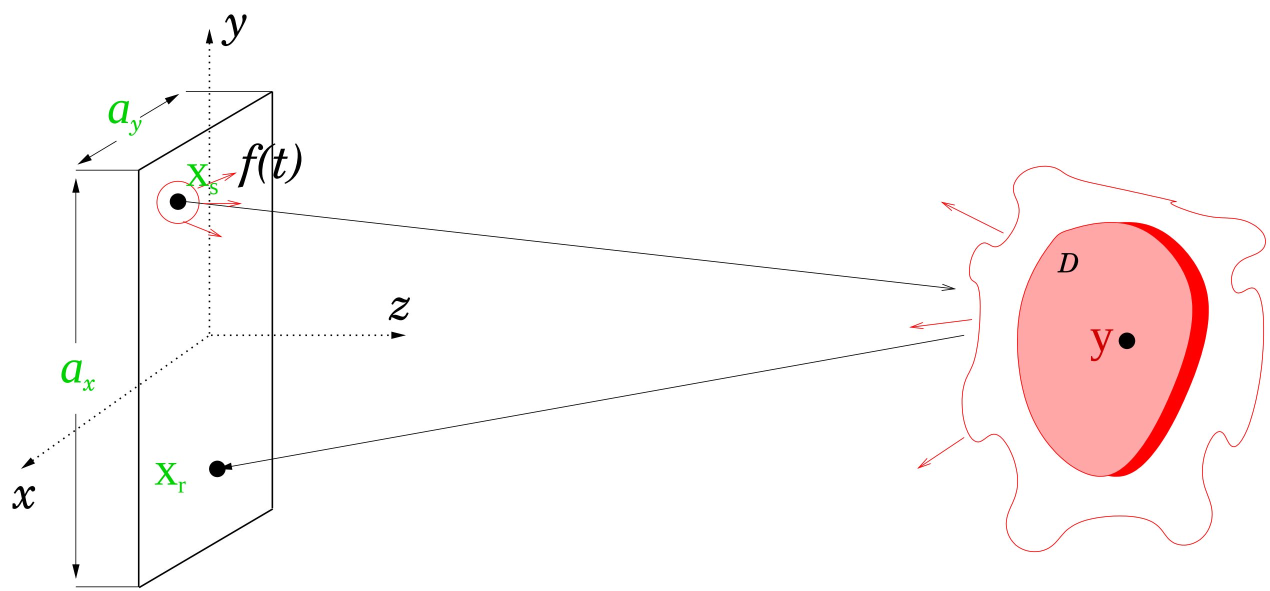

- Objective: recover $\mathcal{D}$ from $P(\mathbf{x}_s, \mathbf{x}_r, t)$ when the background medium is cluttered.
- Application: Imaging underground structures / Non-destructive testing (concrete imaging).

What is the clutter?

- background velocity $c(\mathbf{x})$ consists of a smooth part $c_o(\mathbf{x})$, that is known or can be estimated, and the inhomogeneities (clutter) that cannot be precisely estimated $\Rightarrow$ model as random process.

$$c(\mathbf{x}) = c_0(\mathbf{x}) \left(1 + \sigma\mu\left(\frac{x_1}{l_1}, \frac{x_2}{l_2}\right)\right)$$

- with μ a random process
- l_1, l_2 the correlation lengths (scale of the inhomogeneities)

Velocity profile in the earth

- background velocity $c(\mathbf{x})$ consists of a smooth part $c_o(\mathbf{x})$ (assumed known), and of the fluctuations, which cannot be estimated.

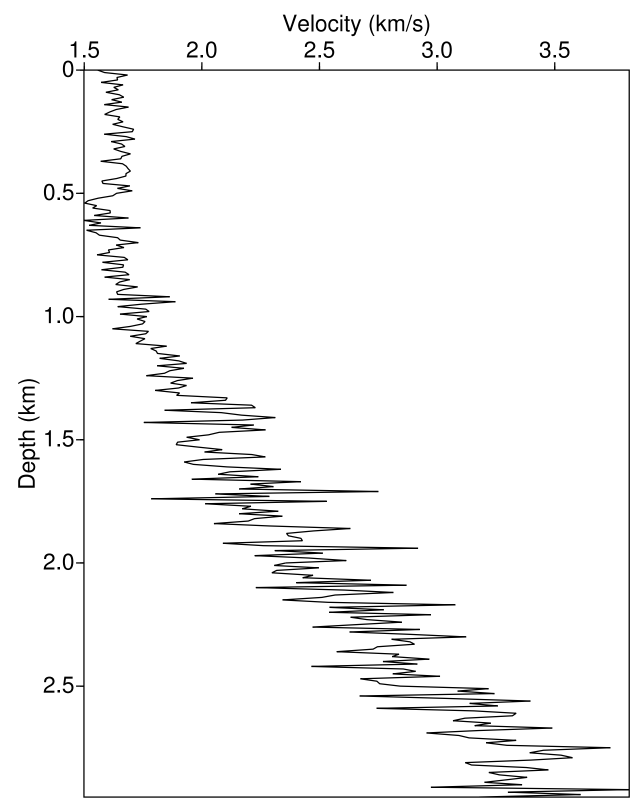

- Velocity profile in a well log

Modeling the clutter

- We assume that the velocity is described by

$$c(\mathbf{x}) = c_0(\mathbf{x})\,(1 + \sigma\mu(\mathbf{x}))$$

- with μ a real valued random process with $< \mu >= 0$ and correlation function:

$$R(\mathbf{x}_1, \mathbf{x}_2) =< \mu(\mathbf{x}_1)\mu(\mathbf{x}_2) >$$

- or by introducing $\overline{\mathbf{x}} = \dfrac{\mathbf{x}_1 + \mathbf{x}_2}{2}, \widetilde{\mathbf{x}} = \mathbf{x}_2 - \mathbf{x}_1$

$$R(\overline{\mathbf{x}}, \widetilde{\mathbf{x}}) =< \mu(\overline{\mathbf{x}} - \widetilde{\mathbf{x}}/2)\mu(\overline{\mathbf{x}} + \widetilde{\mathbf{x}}/2) >$$

- We assume that μ is stationary so that the correlation function depends only on the distance

$$R(\overline{\mathbf{x}}, \widetilde{\mathbf{x}}) = R(\widetilde{\mathbf{x}})$$

Synthetic realization of random media

- on a rectangular grid we generate a filter $F(\mathbf{x})$
- we compute the Fourier transform $\hat{F}(\mathbf{k})$ of $F(\mathbf{x})$
- we generate a white noise distribution $\hat{W}(\mathbf{k})$ ($<\hat{W}>=0$, std=1)
- we compute $\mu(\mathbf{x}) = \mathcal{F}^{-1}(\hat{W}\hat{F})$
- the correlation function of $\mu(\mathbf{x})$ is ($<\overline{\hat{W}(\mathbf{k}_1)}\hat{W}(\mathbf{k}_2)>=\delta(\mathbf{k}_1 - \mathbf{k}_2)$)

$$R(\widetilde{\mathbf{x}}) = (2\pi)^{-d} \int d\mathbf{k} e^{i\mathbf{k}\cdot\widetilde{\mathbf{x}}} \overline{\hat{F}(\mathbf{k})} \hat{F}(\mathbf{k})$$

- we chose F to obtain the desired R

Synthetic realization of random media

- Examples of isotropic clutter correlation functions
- Gaussian $R(|\mathbf{x}_1 - \mathbf{x}_2|) = e^{-\frac{|\mathbf{x}_1 - \mathbf{x}_2|^2}{2l^2}}$
- Power low $R(|\mathbf{x}_1 - \mathbf{x}_2|) = (1 + \dfrac{|\mathbf{x}_1 - \mathbf{x}_2|}{l})e^{-\frac{|\mathbf{x}_1 - \mathbf{x}_2|}{l}}$

Synthetic realization of random media

- 2d example with gaussian correlation fct

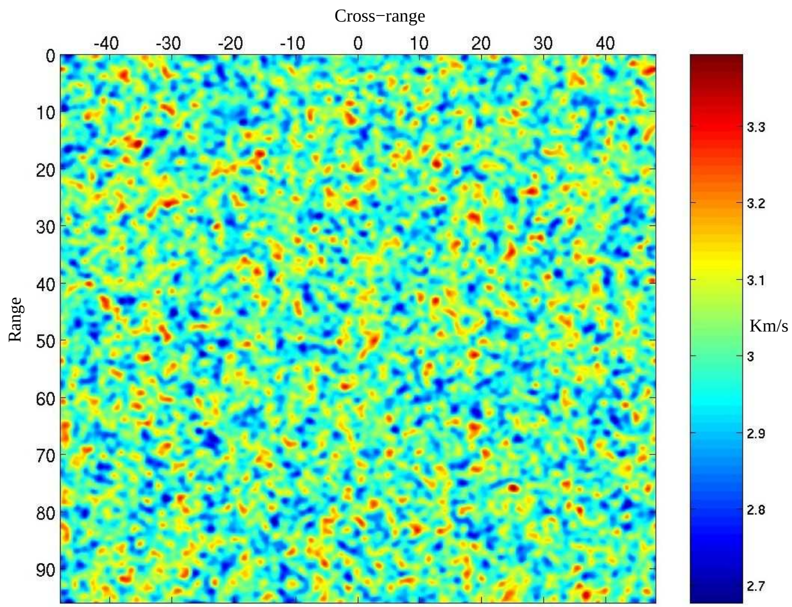

- here the correlation length l is the same in all directions of propagation ($l_{cr} = l_r = l$)

Synthetic realization of random media

- 1d example : Anisotropic (layered) clutter

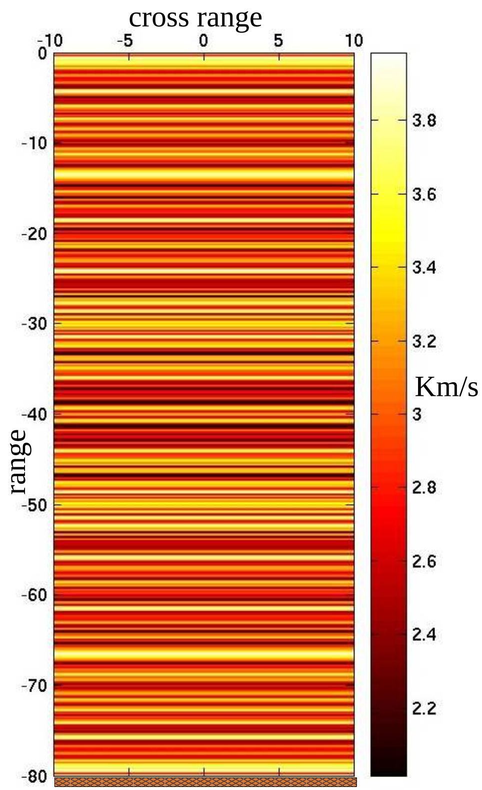

- here the correlation length is infinite in the cross-range direction and finite in the range direction $l_r = l$

The forward model

- Data: $\hat{P}(\mathbf{x}_s, \mathbf{x}_r, \omega) = \hat{f}(\omega)\hat{G}(\mathbf{x}_s, \mathbf{x}_r, \omega)$
- $\hat{G}(\mathbf{x}, \mathbf{y}, \omega)$ satisfying the wave equation

$$\Delta \hat{G}(\mathbf{x}, \mathbf{y}, \omega) + k^2 n^2(\mathbf{x}) \hat{G}(\mathbf{x}, \mathbf{y}, \omega) = -\delta(\mathbf{x} - \mathbf{y}) \text{ in } \mathbb{R}^3$$

- $k = \omega / c_0$: wavenumber
- $n(\mathbf{x}) = c_0 / c(\mathbf{x})$: index of refraction

$$n^2(\mathbf{x}) = n_{BG}^2(\mathbf{x}) + \varrho(\mathbf{x}) + \mu(\mathbf{x})$$

- μ = random part of the refractive index.

The inverse problem

- we can formulate the non-linear least squares problem: Find $\varrho(\mathbf{x})$ by minimizing,

$$J(\varrho) = \int_0^T dt \sum_{\mathbf{x}_s, \mathbf{x}_r} |P(\mathbf{x}_s, \mathbf{x}_r, t) - Q(\mathbf{x}_s, \mathbf{x}_r, t; \varrho)|^2$$

- with $Q(\mathbf{x}_s, \mathbf{x}_r, t; \varrho)$ the data model.
- this is typically not solvable for large array data (as in seismic applications)

Linearized inversion

- Introduce $\hat{G}_B$ solution of

$$\Delta \hat{G}_B(\mathbf{x},\mathbf{y},\omega)+k^2(n_{BG}^2(\mathbf{x})+\mu(\mathbf{x}))\hat{G}_B(\mathbf{x},\mathbf{y},\omega) = -\delta(\mathbf{x}-\mathbf{y}) \text{ in } \mathbb{R}^3$$

- the pressure field is given by,

$$\hat{P}(\mathbf{x},\mathbf{y},\omega) = \hat{f}(\omega)\hat{G}_B(\mathbf{x},\mathbf{y},\omega) + \hat{q}(\mathbf{x},\mathbf{y},\omega)$$

- with $\hat{q}(\mathbf{x},\mathbf{y},\omega)$ solution of,

$$(\Delta + k^2(n_{BG}^2(\mathbf{x}) + \mu(\mathbf{x})))\hat{q}(\mathbf{x},\mathbf{y},\omega) =$$

$$-k^2\varrho(\mathbf{x})(\hat{f}(\omega)\hat{G}_B(\mathbf{x},\mathbf{y},\omega) + \hat{q}(\mathbf{x},\mathbf{y},\omega))$$

Linearized inversion

- So that,

$$\begin{aligned}\hat{q}(\mathbf{x},\mathbf{y},\omega) = & -k^2 \hat{f}(\omega) \int \varrho(\mathbf{z}) \hat{G}_B(\mathbf{x},\mathbf{z},\omega) \hat{G}_B(\mathbf{z},\mathbf{y},\omega) d\mathbf{z} \\ & -k^2 \int \varrho(\mathbf{z}) \hat{q}(\mathbf{x},\mathbf{z},\omega) \hat{G}_B(\mathbf{z},\mathbf{y},\omega) d\mathbf{z}\end{aligned}$$

- Linearization consists in (Born approximation)

$$\hat{q}(\mathbf{x},\mathbf{y},\omega) = -k^2 \hat{f}(\omega) \int \varrho(\mathbf{z}) \hat{G}_B(\mathbf{x},\mathbf{z},\omega) \hat{G}_B(\mathbf{z},\mathbf{y},\omega) d\mathbf{z}$$

Kirchhoff migration

- Let's assume that we know $n^2_{BG}(\mathbf{x})$, $\mu(\mathbf{x}) = 0$.
- The solution of the linearized least squares problem:

$$J(\varrho) = \int d\omega \sum_{\mathbf{x}_s, \mathbf{x}_r} |\hat{P}(\mathbf{x}_s, \mathbf{x}_r, \omega) - \hat{Q}_L(\mathbf{x}_s, \mathbf{x}_r, \omega; \varrho)|^2$$

- with $Q_L(\mathbf{x}_s, \mathbf{x}_r, \omega; \varrho) = \mathcal{A}\varrho$

$$\hat{Q}_L(\mathbf{x}_s, \mathbf{x}_r, \omega; \varrho) = -k^2 \hat{f}(\omega) \int \varrho(\mathbf{z}) \hat{G}_B(\mathbf{x}, \mathbf{z}, \omega) G_B(\mathbf{z}, \mathbf{y}, \omega) d\mathbf{z}$$

- is given by $\varrho = \mathcal{A}^* P(\mathbf{x}_s, \mathbf{x}_r, t)$ because $\mathcal{A}^*\mathcal{A}$ acts as an identity operator on the singularities of ϱ.

Kirchhoff migration

- assuming $n^2_{BG}(\mathbf{x})$ is smooth and using HF assymptotics for the Green's function (neglecting amplitudes) we get that $\mathcal{I}^{\mathsf{KM}}(\mathbf{y}^s)$ gives a good estimate of $\varrho(\mathbf{y}^s)$ (NOTE: we only recover the support - singularities of the function)

$$\mathcal{I}^{\mathsf{KM}}(\mathbf{y}^s) = \sum_{\mathbf{x}_s, \mathbf{x}_r} \int d\omega \hat{P}(\mathbf{x}_s, \mathbf{x}_r, \omega) e^{-i\omega(\tau(\mathbf{x}_s, \mathbf{y}^s) + \tau(\mathbf{y}^s, \mathbf{x}_r))}$$

- $\tau(\mathbf{x}, \mathbf{y})$ is the travel time $\tau(\mathbf{x}, \mathbf{y}) = \min \int \frac{1}{c(X(s))} ds$ where the minimum is over all paths X that start at $\mathbf{x}$ and end at $\mathbf{y}$.

Kirchhoff migration

- references:
  - N. Bleistein, J.K. Cohen, and J.W. Stockwell Jr., *Mathematics of multidimensional seismic imaging, migration, and inversion.* Springer, New York, 2001.
  - G. Beylkin and R. Burridge. *Linearized inverse scattering problems in acoustics and elasticity.* Wave Motion, Vol. 12, No. 1, pp. 15-52, 1990.
  - Lewis and Symes, Inverse Problems, Vol. 7, pp. 597-632, 1991.
  - W. Symes. *Lecture notes in seismic imaging.* Mathematical Geophysics Summer School, Stanford, available at www.trip.caam.rice.edu, 1998.
  - C. Stolk and M. V. de Hoop. *Microlocal analysis of seismic inverse scattering in anisotropic elastic media.* Comm. Pure Appl. Math., Vol. 55, No. 3, pp. 261-301, 2002.
  - C. Stolk and W. Symes. *Smooth objective functionals for seismic velocity inversion.* Inverse Problems, Vol. 19, pp. 73-89, 2003.

Kirchhoff migration resolution

- when $a, B \to \infty \Rightarrow$

$$\mathcal{I}^{\mathrm{KM}}(\mathbf{y}^S) \approx \int_{\mathcal{D}} \delta(\mathbf{y} - \mathbf{y}^S)\varrho(\mathbf{y})d\mathbf{y}$$

  Bleinstein, Cohen, Stockwell (2001)

- for finite a and $B \Rightarrow$
  - range resolution (direction of propagation): $\sigma_{\mathrm{r}} = \dfrac{c_0}{B}$
  - cross-range resolution: $\sigma_{\mathrm{cr}} = \frac{\lambda_0 L}{a}$

The numerical setup

Length scaled by λ_0

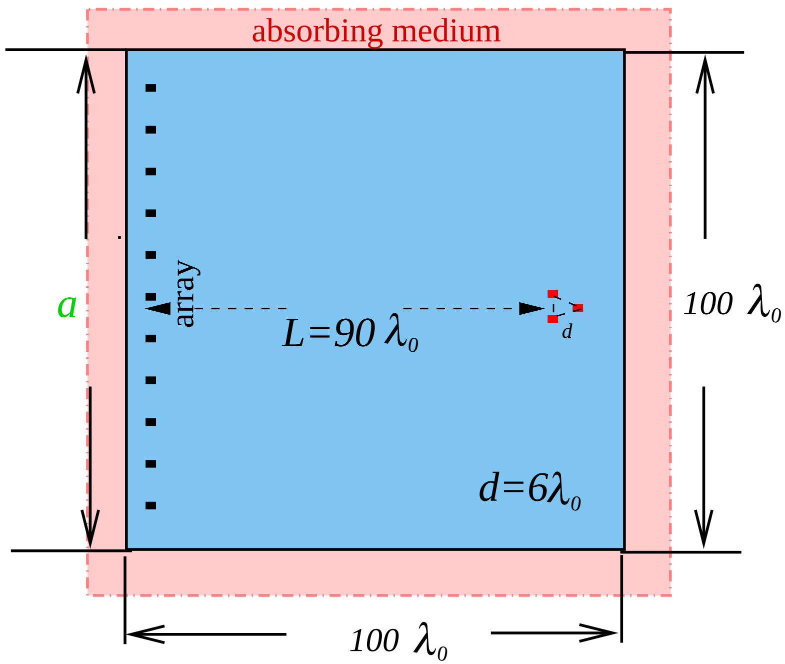

$$\varrho(\mathbf{x})\frac{\partial \mathbf{v}}{\partial t} + \nabla p = 0$$

$$\kappa(\mathbf{x})\frac{\partial p}{\partial t} + \operatorname{div}\mathbf{v} = f(t)\delta(\mathbf{x} - \mathbf{x}_s)$$

$$\varrho(\mathbf{x}) = 1$$

$$\kappa(\mathbf{x}) = \frac{1}{\varrho c^2(\mathbf{x})}$$

- the background velocity is $c_0 = 3km/sec$
- $f(t)$: is the derivative of a gaussian with central frequency $f_0 = 100$KHz and bandwidth $60 - 130$kHz measured at 6dB.

The numerical setup

Length scaled by λ_0

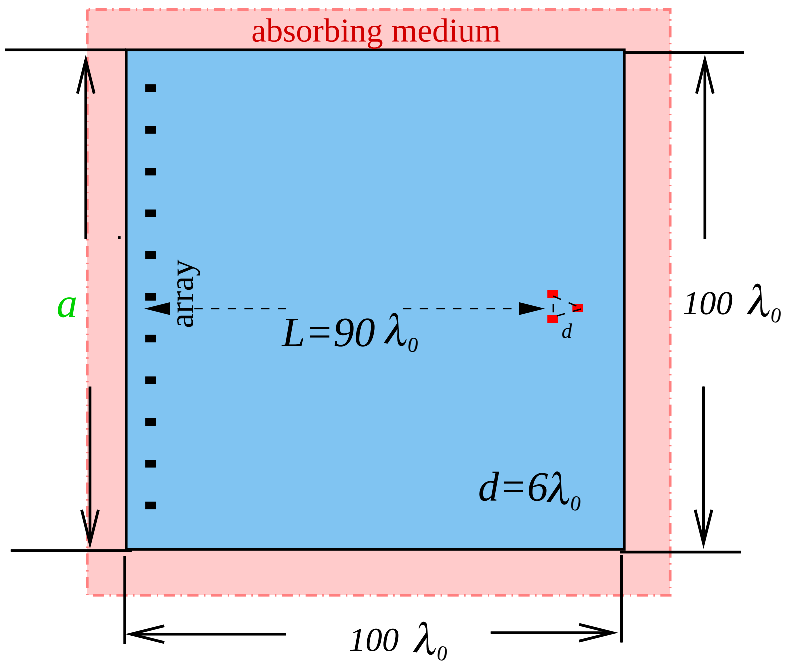

$$\varrho(\mathbf{x})\frac{\partial \mathbf{v}}{\partial t} + \nabla p = 0$$

$$\kappa(\mathbf{x})\frac{\partial p}{\partial t} + \operatorname{div}\mathbf{v} = f(t)\delta(\mathbf{x} - \mathbf{x}_s)$$

$$\varrho(\mathbf{x}) = 1$$

$$\kappa(\mathbf{x}) = \frac{1}{\varrho c^2(\mathbf{x})}$$

- the central wavelength is $\lambda_0 = 3cm$.
- array: 185 elements $\lambda_0/2$ apart, $a = 92\lambda_0$
- the range is $90\lambda_0$

The numerical setup

Length scaled by λ_0

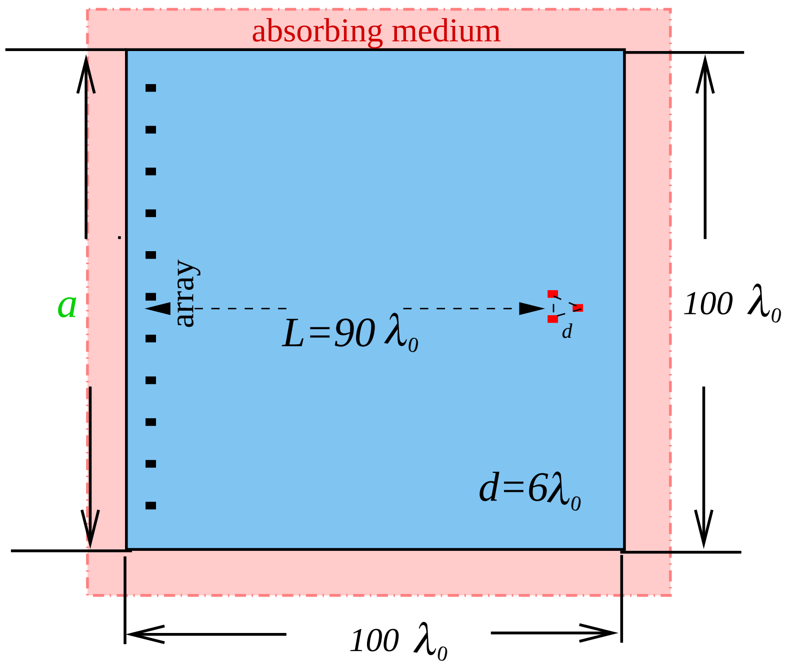

$$\varrho(\mathbf{x})\frac{\partial \mathbf{v}}{\partial t} + \nabla p = 0$$
$$\kappa(\mathbf{x})\frac{\partial p}{\partial t} + \mathrm{div}\mathbf{v} = f(t)\delta(\mathbf{x} - \mathbf{x}_s)$$
$$\varrho(\mathbf{x}) = 1$$
$$\kappa(\mathbf{x}) = \frac{1}{\varrho c^2(\mathbf{x})}$$

- the distance between the objects (sources or targets) is $d = 6\lambda_0$ (or $3\lambda_0$)
- the targets are disks with diameter λ_0.

Data on the array: traces

Passive array

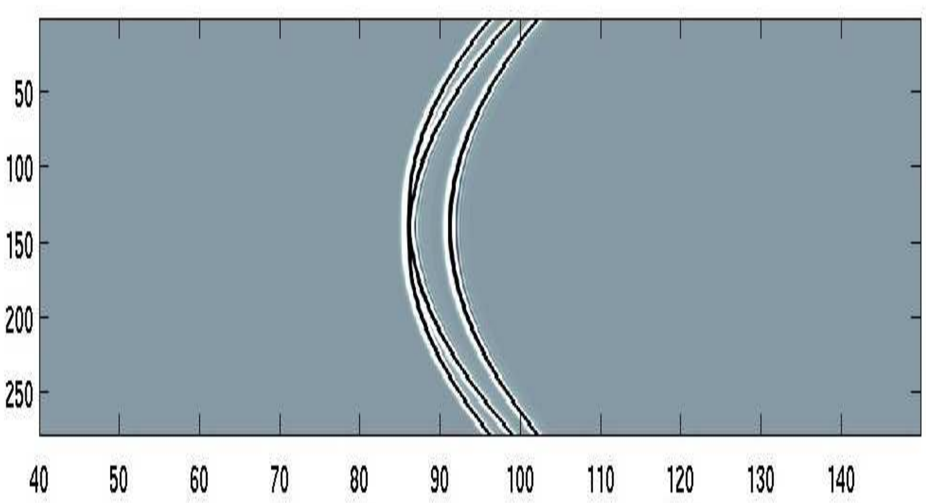

Active array

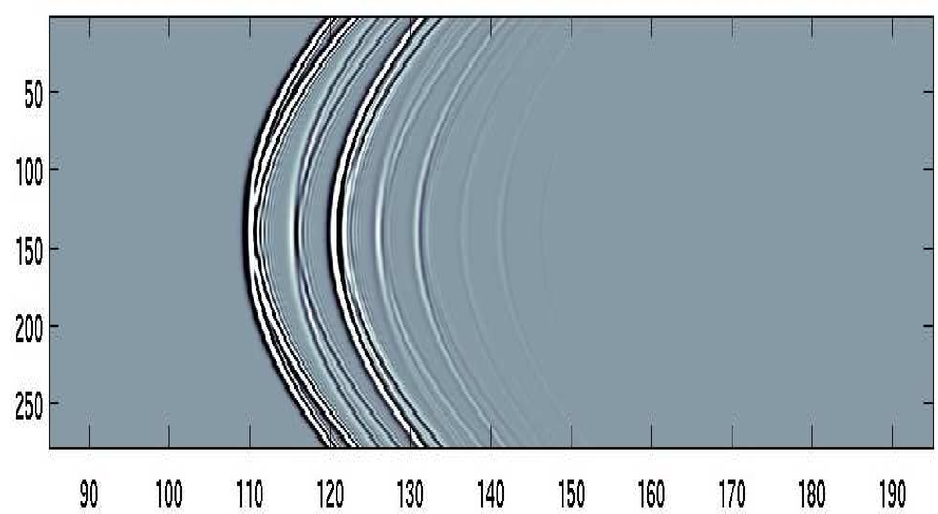

- the cross-range is measured in cm.
- the time is measured in msec.

Kirchhoff migration

- Passive array: imaging functional for KM at $\mathbf{y}^S$

$$\mathcal{I}^{\mathrm{KM}}(\mathbf{y}^s) = \sum_r P(\mathbf{x}_r, \tau(\mathbf{x}_r, \mathbf{y}^S)) = \sum_r \int_B \frac{d\omega}{2\pi} \hat{P}(\mathbf{x}_r, \omega) e^{-i\omega\tau(\mathbf{x}_r, \mathbf{y}^S)}$$

- with $\tau(\mathbf{x}, \mathbf{y}) = |\mathbf{x} - \mathbf{y}|/c_0$ travel time in the known smooth background (here homogeneous)
- Active array: imaging functional for KM at $\mathbf{y}^S$

$$\begin{aligned}\mathcal{I}^{\mathrm{KM}}(\mathbf{y}^s) &= \sum_{r=1}^{N_r} P(\mathbf{x}_s, \mathbf{x}_r, \tau(\mathbf{x}_s, \mathbf{y}^s) + \tau(\mathbf{x}_r, \mathbf{y}^s)) \\ &= \sum_{r=1}^{N_r} \int \frac{d\omega}{2\pi} \hat{P}(\mathbf{x}_s, \mathbf{x}_r, \omega) \overline{G_0(\mathbf{x}_s, \mathbf{y}^s, \omega) G_0(\mathbf{x}_r, \mathbf{y}^s, \omega)}\end{aligned}$$

- with $G_0(\mathbf{x}_s, \mathbf{y}^s, \omega) = e^{i\omega\tau(\mathbf{x}_s, \mathbf{y}^s)}$

Kirchhoff migration results

Passive array

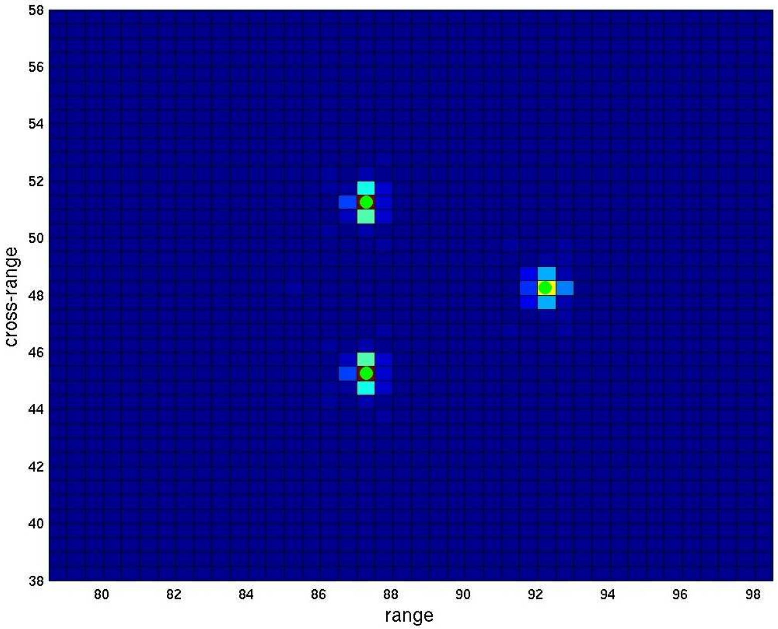

Active array

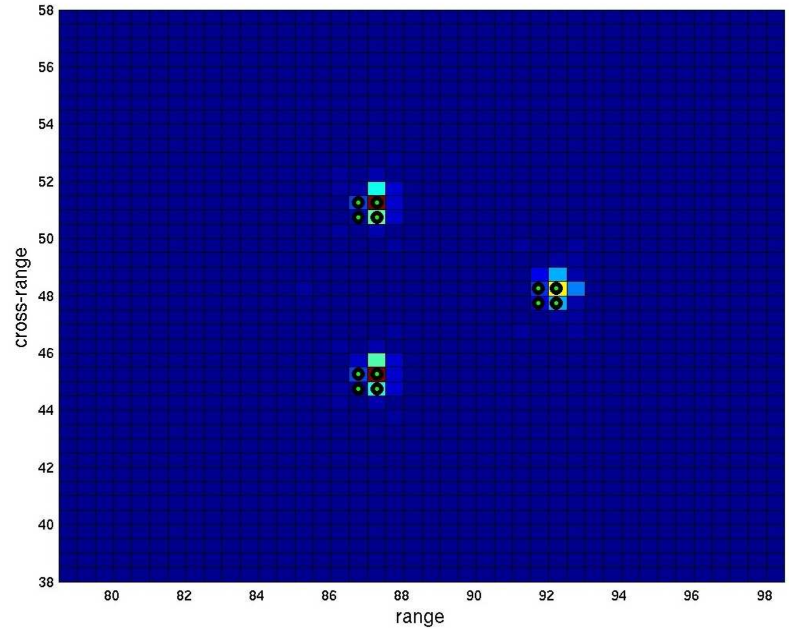

- length is scaled by λ_0
- the search domain is a square $20\lambda_0 \times 20\lambda_0$ centered at the objects
- the pixel size is $\lambda_0/2$.

What happens in clutter?

- Length scaled by λ_0

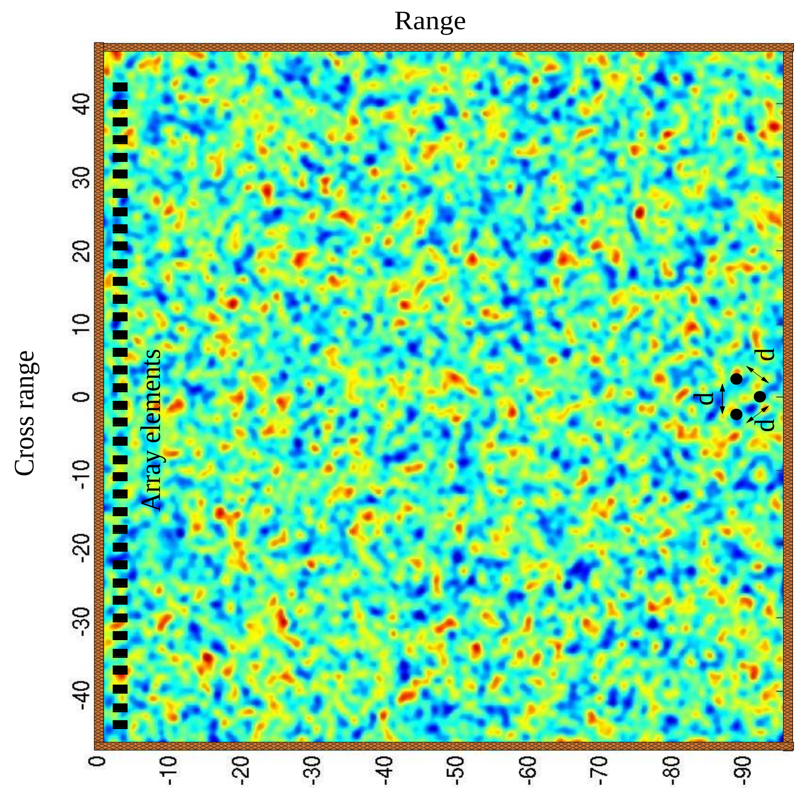

What happens in clutter?

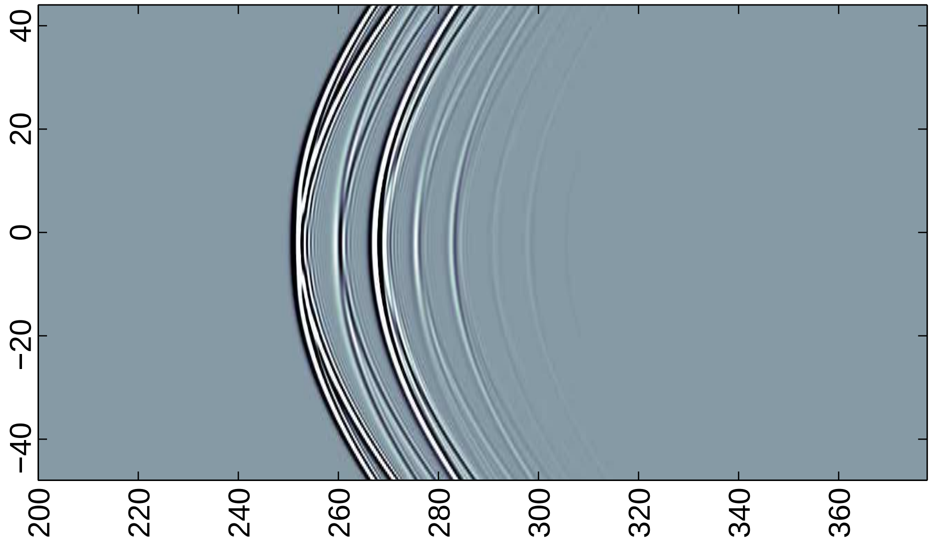

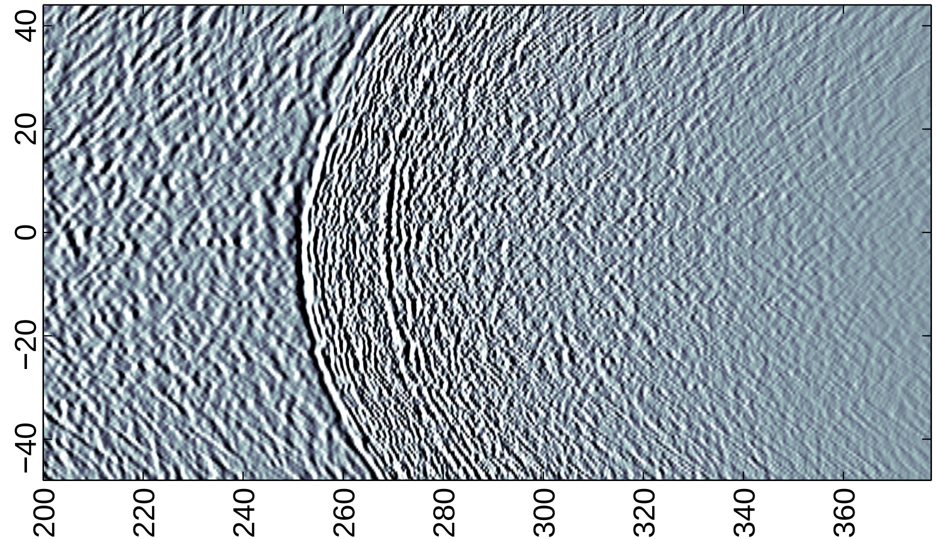

- Length scaled by λ_0 and time by pulsewidth
- the clutter impedes the imaging process as the significant multipathing of the waves by the inhomogeneities results to noisy data traces (the noise is not simply additive)

Migration in clutter

- Classic migration is statisticaly unstable

$$\mathcal{I}^{\mathrm{KM}}(\mathbf{y}^s) = \sum_{r=1}^{N_r} P(\mathbf{x}_s, \mathbf{x}_r, \tau(\mathbf{x}_s, \mathbf{y}^s) + \tau(\mathbf{x}_r, \mathbf{y}^s))$$

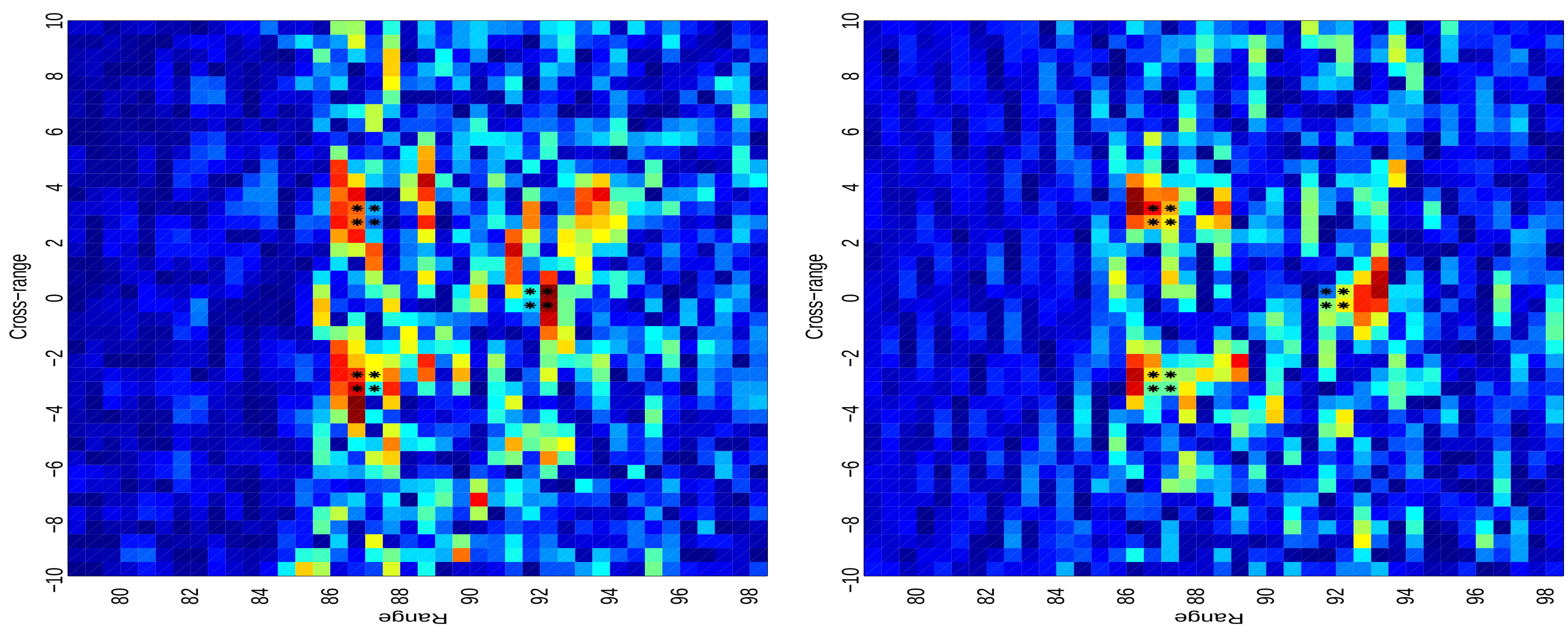

Migration in clutter

- Classic migration is statisticaly unstable

$$\mathcal{I}^{\mathsf{KM}}(\mathbf{y}^s) = \sum_{r=1}^{N_r} P(\mathbf{x}_s, \mathbf{x}_r, \tau(\mathbf{x}_s, \mathbf{y}^s) + \tau(\mathbf{x}_r, \mathbf{y}^s))$$

- To make migration work we should remove the delay spread:
  - ✗ trace denoising ? (noise is not additive)
  - ✔ we use time-reversal based techniques

Migration in frequency domain

- the migration functional

$$\mathcal{I}^{\text{KM}}(\mathbf{y}^s) = \sum_{r=1}^{N_r} P(\mathbf{x}_s, \mathbf{x}_r, \tau(\mathbf{x}_s, \mathbf{y}^s) + \tau(\mathbf{x}_r, \mathbf{y}^s))$$

- can be written as

$$\mathcal{I}^{\text{KM}}(\mathbf{y}^s) = \sum_{r=1}^{N_r} \int d\omega \hat{P}(\mathbf{x}_s, \mathbf{x}_r, \omega) \overline{G_0(\mathbf{x}_s, \mathbf{y}^s, \omega) G_0(\mathbf{x}_r, \mathbf{y}^s, \omega)}$$

- with $G_0(\mathbf{x}_s, \mathbf{y}^s, \omega) = e^{i\omega\tau(\mathbf{x}_s, \mathbf{y}^s)}$

Coherent interferometry (CINT)

- an ideal way to image would be to backpropagate with the exact $G(\mathbf{x}_s, \mathbf{y}^s, \omega)$. This is called time reversal and has two fundemental properties in clutter:
  - ✔ statistical stability
  - ✔ super-resolution
- But we do not know the clutter ! ($G(\mathbf{x}_s, \mathbf{y}^s, \omega)$ is unknow)

Coherent interferometry (CINT)

- we cross-correlate the traces locally in space and time:
  - cross-correlation in space is limitted by the decoherence length X_d
  - cross-correlation in time is limitted by the delay spread T_d
- we call these local cross-corelations coherent interferograms
- CINT consists in migrating the coherent interferograms to the search point $\mathbf{y}^s$ using $G_0(\mathbf{x}_s, \mathbf{y}^s, \omega)$

CINT imaging functional

$$\mathcal{I}^{\text{CINT}}(\mathbf{y}^s;\Omega_d,\kappa_d) \sim \int_{\overline{\omega}\in B} d\overline{\omega} \int_{\overline{\mathbf{x}}\in a} d\overline{\mathbf{x}} \int d\tilde{\omega}\ \hat{\Psi}(\tilde{\omega};\Omega_d) \int d\widetilde{\mathbf{x}}\ \hat{\Phi}\left(\frac{\overline{\omega}}{c_0}\widetilde{\mathbf{x}};\kappa_d^{-1}\right)$$

$$\hat{P}\left(\overline{\mathbf{x}}+\tfrac{\widetilde{\mathbf{x}}}{2},\mathbf{x}_s,\overline{\omega}+\tfrac{\tilde{\omega}}{2}\right)\exp\left\{-i(\overline{\omega}+\tfrac{\tilde{\omega}}{2})\left[\tau(\overline{\mathbf{x}}+\tfrac{\widetilde{\mathbf{x}}}{2},\mathbf{y}^s)+\tau(\mathbf{x}_s,\mathbf{y}^s)\right]\right\}$$

$$\overline{\hat{P}\left(\overline{\mathbf{x}}-\tfrac{\widetilde{\mathbf{x}}}{2},\mathbf{x}_s,\overline{\omega}-\tfrac{\tilde{\omega}}{2}\right)}\exp\left\{+i(\overline{\omega}-\tfrac{\tilde{\omega}}{2})\left[\tau(\overline{\mathbf{x}}-\tfrac{\widetilde{\mathbf{x}}}{2},\mathbf{y}^s)+\tau(\mathbf{x}_s,\mathbf{y}^s)\right]\right\}$$

using the midpoint and offset variables

$$\overline{\mathbf{x}}=\frac{\mathbf{x}_r+\mathbf{x}_r{}'}{2},\widetilde{\mathbf{x}}=\mathbf{x}_r-\mathbf{x}_r{}'\ ;\ \overline{\omega}=\frac{\omega+\omega'}{2},\tilde{\omega}=\omega-\omega'$$

CINT imaging functional

$$
\mathcal{I}^{\mathsf{CINT}}(\mathbf{y}^s;\Omega_d,\kappa_d) \sim \int_{\overline{\omega}\in B} d\overline{\omega} \int_{\overline{\mathbf{x}}\in a} d\overline{\mathbf{x}} \int d\tilde{\omega}\ \hat{\Psi}(\tilde{\omega};\Omega_d) \int d\widetilde{\mathbf{x}}\ \hat{\Phi}\left(\frac{\overline{\omega}}{c_0}\widetilde{\mathbf{x}};\kappa_d^{-1}\right)
$$

$$
\hat{P}\left(\overline{\mathbf{x}}+\tfrac{\widetilde{\mathbf{x}}}{2},\mathbf{x}_s,\overline{\omega}+\tfrac{\tilde{\omega}}{2}\right)\exp\left\{-i(\overline{\omega}+\tfrac{\tilde{\omega}}{2})\left[\tau(\overline{\mathbf{x}}+\tfrac{\widetilde{\mathbf{x}}}{2},\mathbf{y}^s)+\tau(\mathbf{x}_s,\mathbf{y}^s)\right]\right\}
$$

$$
\overline{\hat{P}\left(\overline{\mathbf{x}}-\tfrac{\widetilde{\mathbf{x}}}{2},\mathbf{x}_s,\overline{\omega}-\tfrac{\tilde{\omega}}{2}\right)}\exp\left\{+i(\overline{\omega}-\tfrac{\tilde{\omega}}{2})\left[\tau(\overline{\mathbf{x}}-\tfrac{\widetilde{\mathbf{x}}}{2},\mathbf{y}^s)+\tau(\mathbf{x}_s,\mathbf{y}^s)\right]\right\}
$$

- $\tilde{\omega}$ is restricted by window $\hat{\Psi}$ to $|\tilde{\omega}| \leq \Omega_d$, with Ω_d the decoherence frequency $(\sim 1/T_d)$
- $\widetilde{\mathbf{x}}$ is restricted by window $\hat{\Phi}$ to $|\widetilde{\mathbf{x}}| \leq X_d(\overline{\omega})$, with $X_d(\overline{\omega})$ the decoherence length (the TR spot size at frequency $\overline{\omega}$). The support of $\hat{\Phi}$ is $\kappa_d^{-1} = \overline{\omega}X_d(\overline{\omega})/c_0$

CINT and statistical smoothing

- for small $|\widetilde{\mathbf{x}}|$ we can linearize the phase

$$\exp\left\{-i\overline{\omega}\left[\tau\big(\overline{\mathbf{x}}+\tfrac{\widetilde{\mathbf{x}}}{2},\mathbf{y}^s\big)-\tau\big(\overline{\mathbf{x}}-\tfrac{\widetilde{\mathbf{x}}}{2},\mathbf{y}^s\big)\right]\right\}\approx\exp\left\{-i\overline{\omega}\widetilde{\mathbf{x}}\cdot\nabla_{\overline{\mathbf{x}}}\tau\big(\overline{\mathbf{x}},\mathbf{y}^s\big)\right\}$$

$$\exp\left\{-i\tilde{\omega}\left[\tau\big(\overline{\mathbf{x}}+\tfrac{\widetilde{\mathbf{x}}}{2},\mathbf{y}^s\big)+\tau\big(\overline{\mathbf{x}}-\tfrac{\widetilde{\mathbf{x}}}{2},\mathbf{y}^s\big)\right]\right\}\approx\exp\left\{-i2\tilde{\omega}\tau\big(\overline{\mathbf{x}},\mathbf{y}^s\big)\right\}$$

CINT and statistical smoothing

- the imaging functional becomes

$$\mathcal{I}^{\text{CINT}}(\mathbf{y}^S;\Omega_d,\kappa_d) = \int dt \int d\mathbf{k}\Phi(c_0\nabla_{\overline{\mathbf{x}}}\tau(\overline{\mathbf{x}},\mathbf{y}^s) - \mathbf{k};\kappa_d)$$
$$\Psi(\tau(\overline{\mathbf{x}},\mathbf{y}^s) + \tau(\mathbf{x}_s,\mathbf{y}^s) - t; T_d) \int d\overline{\omega} W(\overline{\mathbf{x}}, \frac{\overline{\omega}}{c_0}\mathbf{k}, t),$$

- with $W(\cdot)$ the Wigner distribution of the data

$$W(\overline{\mathbf{x}}, \frac{\overline{\omega}}{c_0}\mathbf{k}, t) = \int d\tilde{\omega} \int \frac{d\widetilde{\mathbf{x}} e^{-i\tilde{\omega}t - i\frac{\overline{\omega}}{c_0}\widetilde{\mathbf{x}}\cdot\mathbf{k}} \hat{P}\left(\overline{\mathbf{x}} + \frac{\widetilde{\mathbf{x}}}{2}, \mathbf{x}_s, \overline{\omega} + \frac{\tilde{\omega}}{2}\right)}{\hat{P}\left(\overline{\mathbf{x}} - \frac{\widetilde{\mathbf{x}}}{2}, \mathbf{x}_s, \overline{\omega} - \frac{\tilde{\omega}}{2}\right)}$$

- $W(\cdot)$ is highly fluctuating but decorrelates rapidly in $\overline{\omega}$ and $\mathbf{k}$
  $\rightsquigarrow$ in CINT we have stability by smoothing

CINT as smooth migration

- CINT can be also written as

$$\mathcal{I}^{\text{CINT}}(\mathbf{y}^S;\Omega_d,\kappa_d) = \int d\overline{\mathbf{x}} \int d\widetilde{\mathbf{x}} \left[P\left(\overline{\mathbf{x}} + \frac{\widetilde{\mathbf{x}}}{2}, \mathbf{x}_s, t + \frac{\mathbf{k}\cdot\widetilde{\mathbf{x}}}{2c_0}\right) P\left(\overline{\mathbf{x}} - \frac{\widetilde{\mathbf{x}}}{2}, \mathbf{x}_s, t - \frac{\mathbf{k}\cdot\widetilde{\mathbf{x}}}{2c_0}\right)\right] \star_{\mathbf{k}} \Phi(\mathbf{k};\kappa_d)\big|_{\mathbf{k}=c_0\nabla_{\overline{\mathbf{x}}}\tau(\overline{\mathbf{x}},\mathbf{y}^s)} \star_t \Psi(t;T_d)\big|_{t=\tau(\overline{\mathbf{x}},\mathbf{y}^s)+\tau(\mathbf{x}_s,\mathbf{y}^s)}$$

- when Φ, Ψ are δ functions (no smoothing) we obtain

$$\mathcal{I}^{\text{CINT}}(\mathbf{y}^S;\Omega_d,\kappa_d) = \left[\mathcal{I}^{\text{KM}}(\mathbf{y}^s)\right]^2$$

- CINT is a statistically stable smoothed migration method !

CINT as smooth migration

- CINT can be also written as

$$\mathcal{I}^{\text{CINT}}(\mathbf{y}^S;\Omega_d,\kappa_d) = \int d\overline{\mathbf{x}} \int d\widetilde{\mathbf{x}} \Bigg[P\left(\overline{\mathbf{x}} + \frac{\widetilde{\mathbf{x}}}{2}, \mathbf{x}_s, t + \frac{\mathbf{k}\cdot\widetilde{\mathbf{x}}}{2c_0}\right) P\left(\overline{\mathbf{x}} - \frac{\widetilde{\mathbf{x}}}{2}, \mathbf{x}_s, t - \frac{\mathbf{k}\cdot\widetilde{\mathbf{x}}}{2c_0}\right)\Bigg]$$

$$\star_{\mathbf{k}}\ \Phi(\mathbf{k};\kappa_d)\big|_{\mathbf{k}=c_0\nabla_{\overline{\mathbf{x}}}\tau(\overline{\mathbf{x}},\mathbf{y}^s)} \star_t\ \Psi(t;T_d)\big|_{t=\tau(\overline{\mathbf{x}},\mathbf{y}^s)+\tau(\mathbf{x}_s,\mathbf{y}^s)}$$

- Smoothing over arrival time by convolution with $\Psi(t;T_d)$ of support $T_d \approx 1/\Omega_d$ affects range resolution c_0/Ω_d.
- Smoothing in direction of arrival by convol. with $\Phi(\mathbf{k};\kappa_d)$ with supp. in ball of radius $\kappa_d \rightsquigarrow$ cross range resolution $L\kappa_d \approx \lambda_0 L/X_d(\omega_0)$.

Resolution summary

- migration resolution in homogeneous media
  - in range : $O\left(\frac{c_0}{B}\right)$
  - in cross-range : $O\left(\lambda\frac{L}{a}\right) = O\left(\frac{c_0 L}{\omega_0 a}\right)$
- CINT resolution in clutter ($\Omega_d < B$ & $X_d < a$)
  - in range : $O\left(\frac{c_0}{\Omega_d}\right)$
  - in cross-range : $O\left(L\kappa_d\right) = O\left(\frac{c_0 L}{\omega_0 X_d(\omega_0)}\right)$
- for $\Omega_d \ll B$ & $X_d \ll a$
  - ✔ incoherent imaging should be used (diffusion)

$$D = \frac{c_0 l^*}{3}$$

  - CINT works for $L < l^*$ (in numerics $l^* = 75\lambda_0$)

Adaptive CINT

- How can we find Ω_d and κ_d ?
- We may derive (theoretical) formulae for Ω_d and κ_d. But this will be model dependent.
- We can estimate the decoherence parameters using statistical data processing techniques, but this can be tricky.
- We found that a more efficient approach is to do an adaptive estimation of the smoothing parameters, during the image formation process.

Adaptive CINT

- View the imaging function as $\mathcal{I}^{\text{CINT}}(\mathbf{y}^s; \Omega_d, \kappa_d)$ and seek parameters Ω_d and κ_d by achieving an optimal balance between statistical smoothing and resolution.
- Penalize the speckles (left image) by using a norm of the gradient. To obtain a tight image, we should also penalize the blur (see right image) by using a sparsity measure. The "optimal" result is given in the middle.

$X_d = a, \Omega_d = B$ $\quad$ $X_d = X_d^*, \Omega_d = \Omega_d^*$ $\quad$ $X_d < X_d^*, \Omega_d < \Omega_d^*$

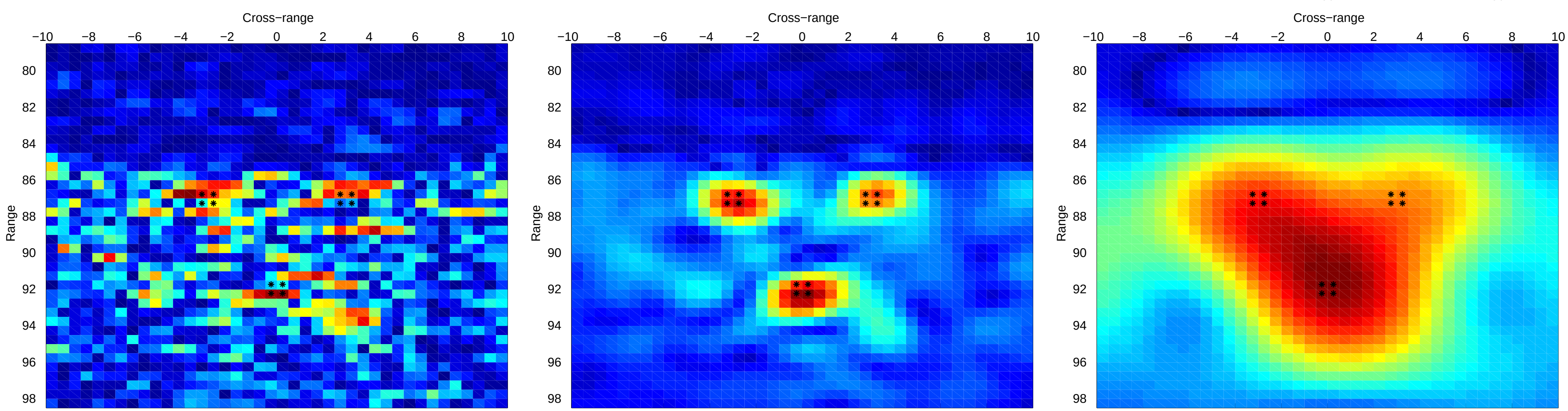

Adaptive CINT

- Ω_d and κ_d are determined by minimizing $\mathcal{O}(\mathbf{y}^s; \Omega_d, \kappa_d) = \|\mathcal{J}_{\mathcal{N}}(\mathbf{y}^s; \Omega_d, \kappa_d)\|_{L^1(\mathcal{D})} + \alpha \, \|\nabla_{\mathbf{y}^s} \mathcal{J}_{\mathcal{N}}(\mathbf{y}^s; \Omega_d, \kappa_d)\|_{L^1(\mathcal{D})}$,
- with $\mathcal{J}_{\mathcal{N}}(\mathbf{y}^s) = \sqrt{|\mathcal{J}(\mathbf{y}^s)|} / \sup_{\mathbf{y}^s \in \mathcal{D}_s} \sqrt{|\mathcal{J}(\mathbf{y}^s)|}$
- for point targets we use $\alpha = 1$

Adaptive CINT

- Ω_d and κ_d are determined by minimizing
$\mathcal{O}(\mathbf{y}^s; \Omega_d, \kappa_d) =$
$\left\| \mathcal{J}_{\mathcal{N}}(\mathbf{y}^s; \Omega_d, \kappa_d) \right\|_{L^1(\mathcal{D})} + \alpha \left\| \nabla_{\mathbf{y}^s} \mathcal{J}_{\mathcal{N}}(\mathbf{y}^s; \Omega_d, \kappa_d) \right\|_{L^1(\mathcal{D})},$
- This is very different from usual denoising,
$$\|\mathcal{N}(\mathbf{y}^s) - \mathcal{I}(\mathbf{y}^s)\|_{\mathrm{prox}} + \alpha \|\mathcal{I}(\mathbf{y}^s)\|_{\mathrm{reg}}$$
- where $\mathcal{N}$ is a given noisy image, $\mathcal{I}$ is the desired denoised image, $\|\cdot\|_{\mathrm{prox}}$ is a proximity norm, usually $L^2(D)$, and$\|\cdot\|_{reg}$ is a regularization norm, usually TV.
- We do not have an image $\mathcal{N}$ so there is no proximity norm part. We use instead the L^1 norm of the image which is small, when the image is sparse. We do have however the regularization term.

Adaptive CINT results I

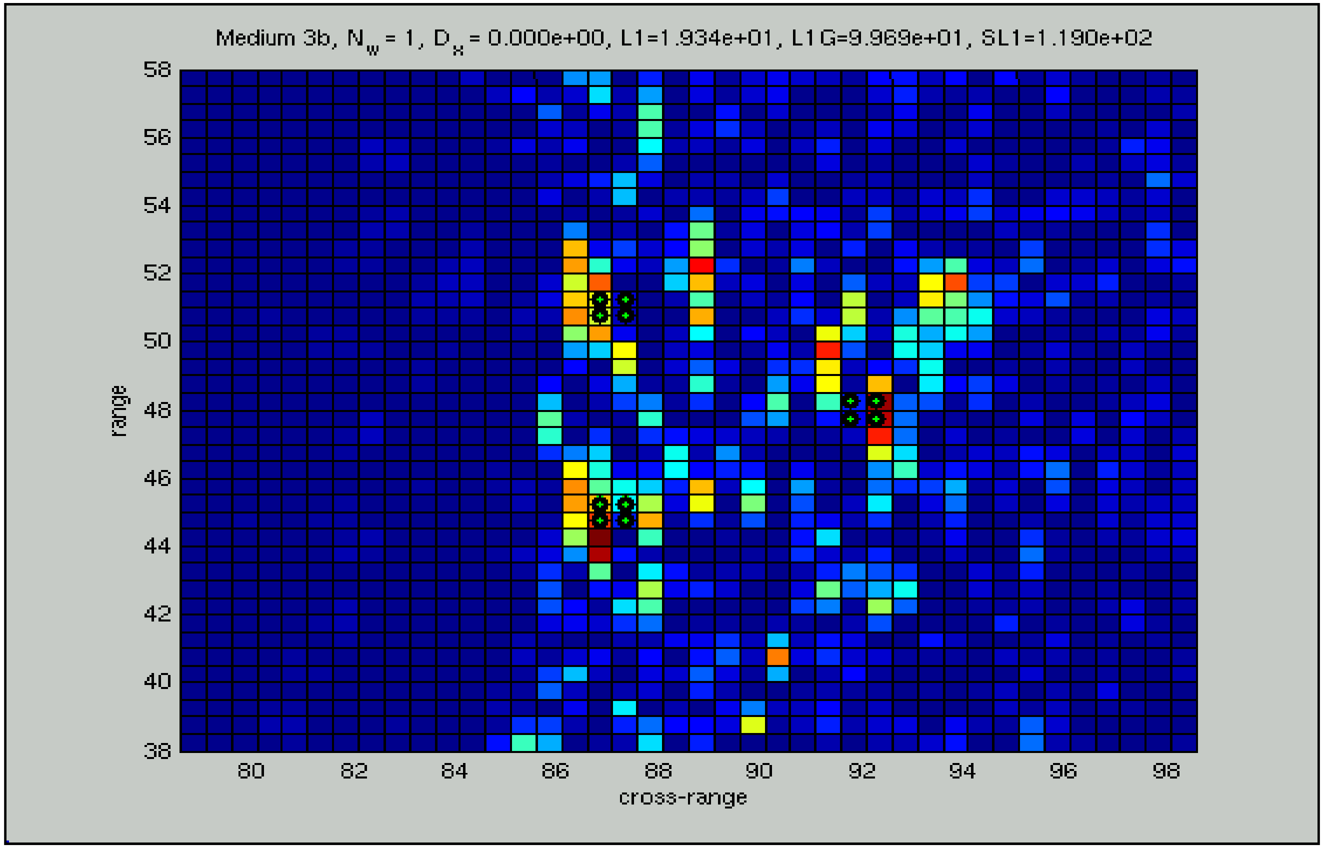

- We use the NOMADm software package (C. Audet, J. Dennis, M. Abramson), that uses a mesh-adaptive direct search method for constrained, nonlinear, mixed variable problems.

Adaptive CINT Results II

IMAGE SEGMENTATION

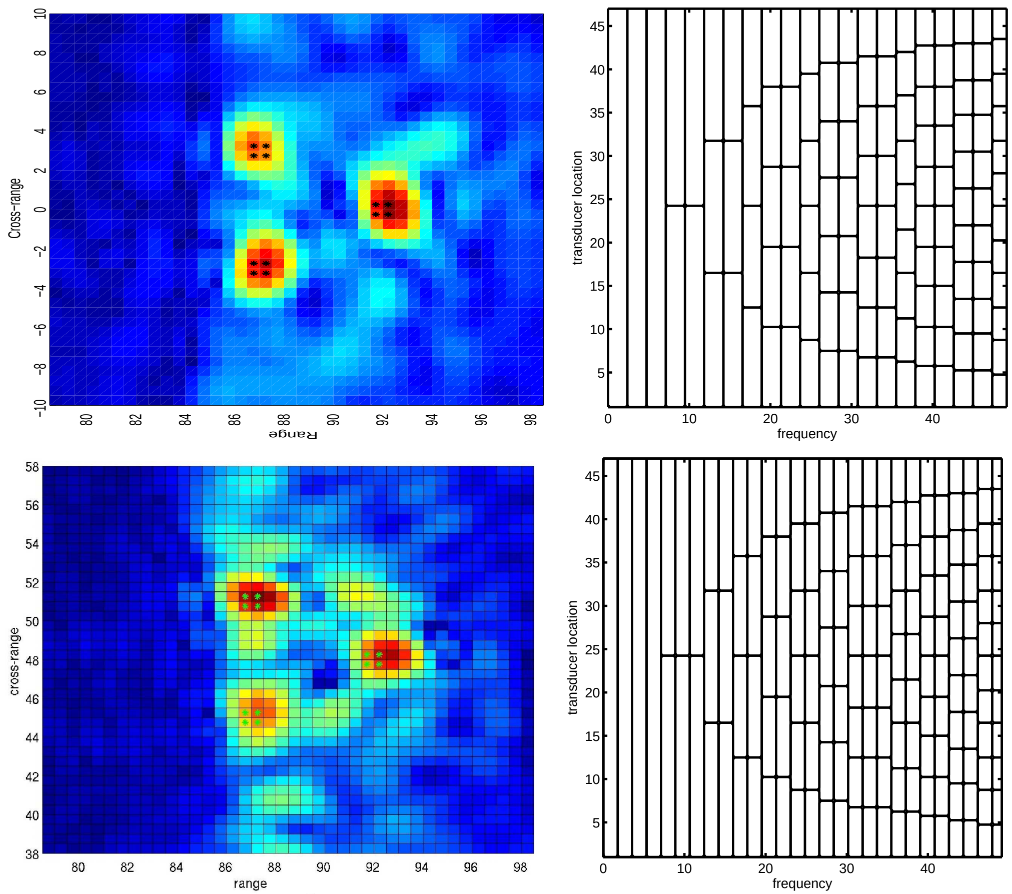

Top: mono-scale, Bottom: multi-scale random medium with standard deviation 3%.

Anisotropic clutter

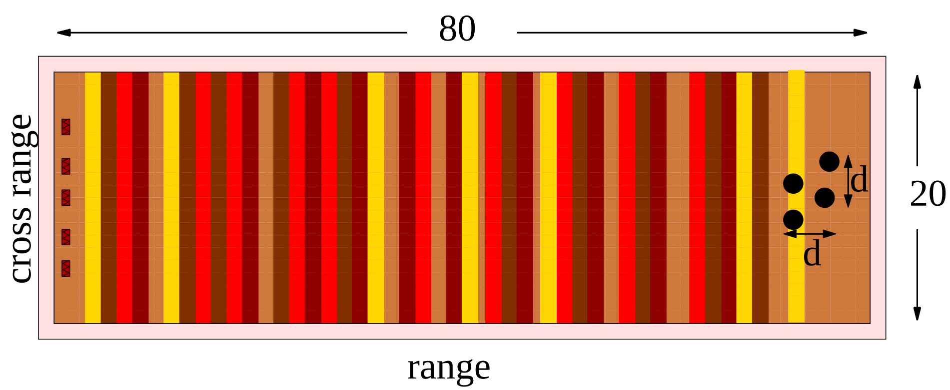

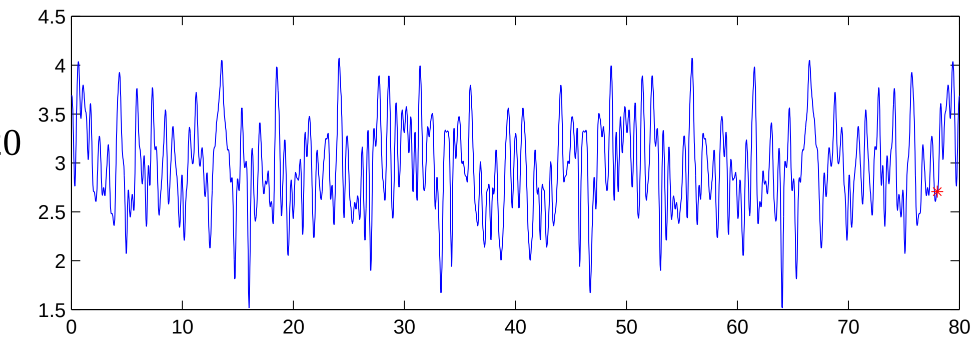

- $c_0 = 3$Km/s, $B = 0.6 - 1.3$ KHz, $\lambda_0 = 3$m
- $l = \lambda_0/10$, $L = 80\lambda_0 = 800l$
- strong fluctuations std $s = 30\%$,
- In this regime we have pulse stabilization (ODA) and in the limit $\lambda_0/L = \epsilon \to 0$ KM is stable
- CINT here is obtained using only window $\Psi(t; T_d)$, i.e $\Phi(\kappa; \kappa_d)$ is a δ function

Anisotropic clutter: traces

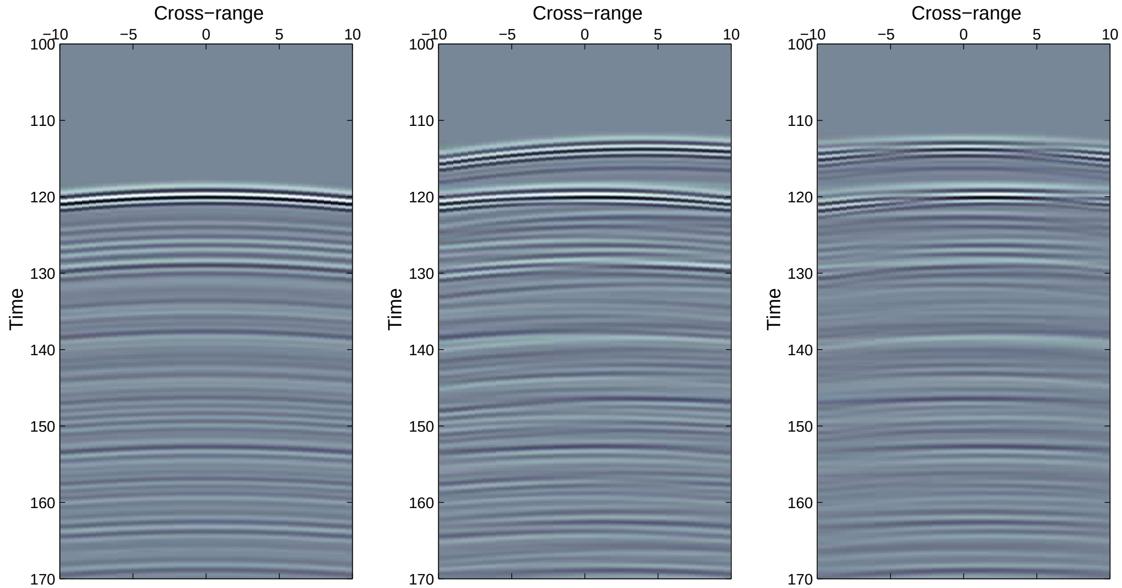

- The ordinate in the pictures is time scaled by the pulse-width and the abscissa is the array element position in λ_0.

Anisotropic clutter: KM vs CINT

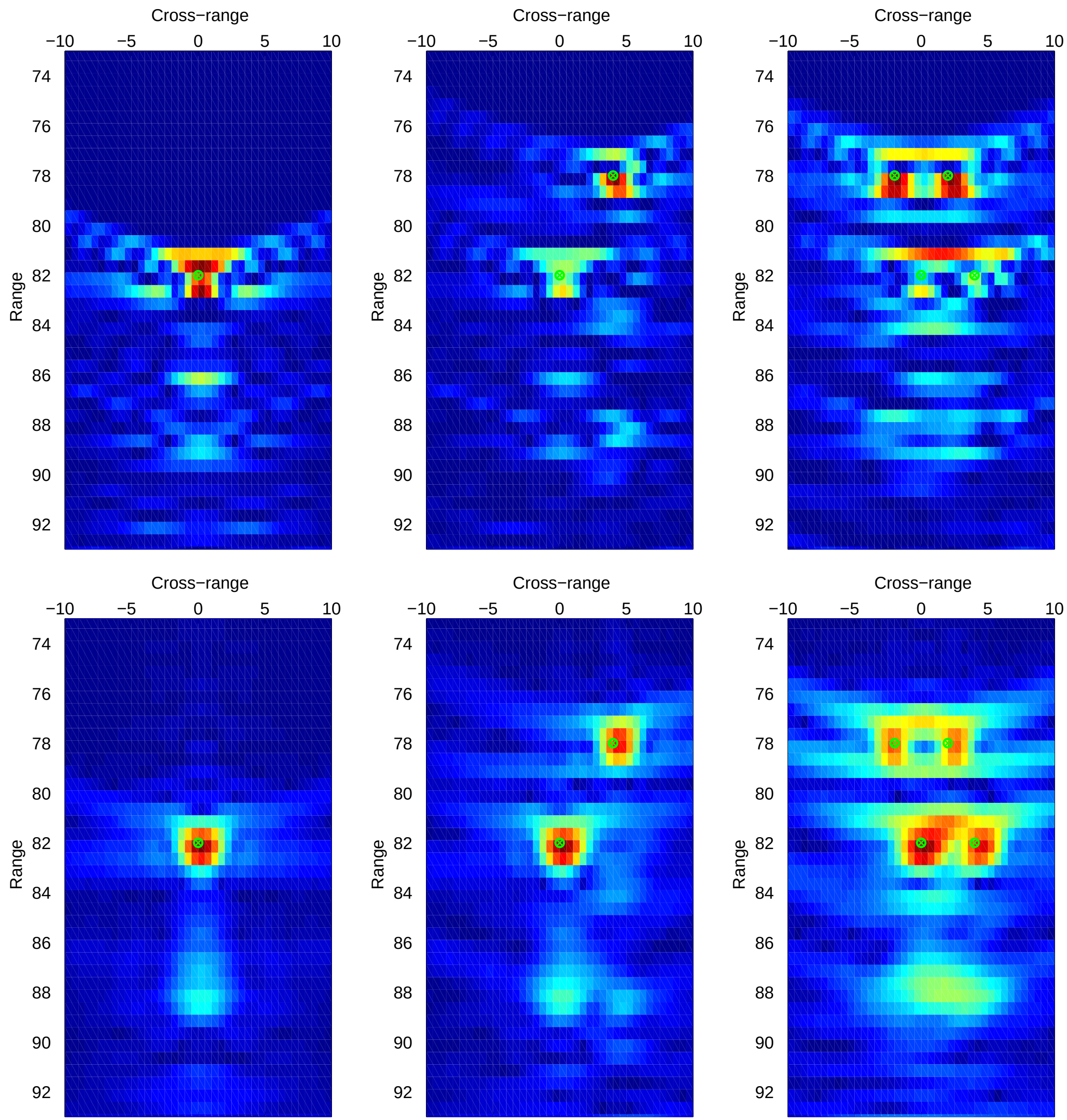

References

- Finely Layered media

  - M. Asch, W. Kohler, G. Papanicolaou, M. Postel, and B. White, Frequency content of randomly scattered signals, SIAM Rev., 33 (1991), pp. 519-625.
  - J. F. Clouet and J. P. Fouque, Spreading of a pulse travelling in random media, Ann. Appl. Probab., 4 (1994), pp. 1083-1097.
  - J. Chillan and J. P. Fouque, Pressure fields generated by acoustical pulses propagating in randomly layered media, SIAM J. Appl. Math., 58 (1998), pp. 1532-1546.
  - J. P. Fouque, S. Garnier, A. Nachbin, and K. Solna, Time-reversal refocusing for point source in randomly layered media, Wave Motion, 42 (2005), pp. 238-260.
  - J. Garnier, Imaging in randomly layered media by cross-correlating noisy signals, Multiscale Model. Simul., 4 (2005), pp. 610-640.
  - L. Borcea, G. Papanicolaou and CT, Coherent interferometry in finely layered random media, SIAM Journal on Multiscale Modeling and Simulation, vol 5, (2006), pp. 62 - 83.
  - L. Borcea, G. Papanicolaou and CT, Coherent Interferometric Imaging, to appear in "Geophysics", 2006.

References

- Isotropic clutter

  - L. Borcea, G. Papanicolaou and CT, Theory and applications of time reversal and interferometric imaging, Inverse Problems, vol 19, (2003), pp. 5139-5164.
  - L. Borcea, G. Papanicolaou and CT, Interferometric array imaging in clutter, Inverse Problems, vol 21, (2005), pp. 1419-1460.
  - L. Borcea, G. Papanicolaou and CT, Adaptive interferometric imaging in clutter and optimal illumination, to appear in Inverse Problems, 2006.
  - G. Bal, G. Papanicolaou and L. Ryzhik, Self-averaging in time reversal for the parabolic wave equation, Stochastics and Dynamics, 2, (2002), pp. 507-531.
  - G. Bal and L. Ryzhik, Time reversal and refocusing in random media: SIAM Journal on Applied Mathematics, 63 (2003), 1475 -1498.
  - G. Papanicolaou, L. Ryzhik and K. Solna, Statistical stability in time reversal, SIAM J. on Appl. Math., 64 (2004), pp. 1133-1155.

Real data: measurements

- Concrete structure to be imaged

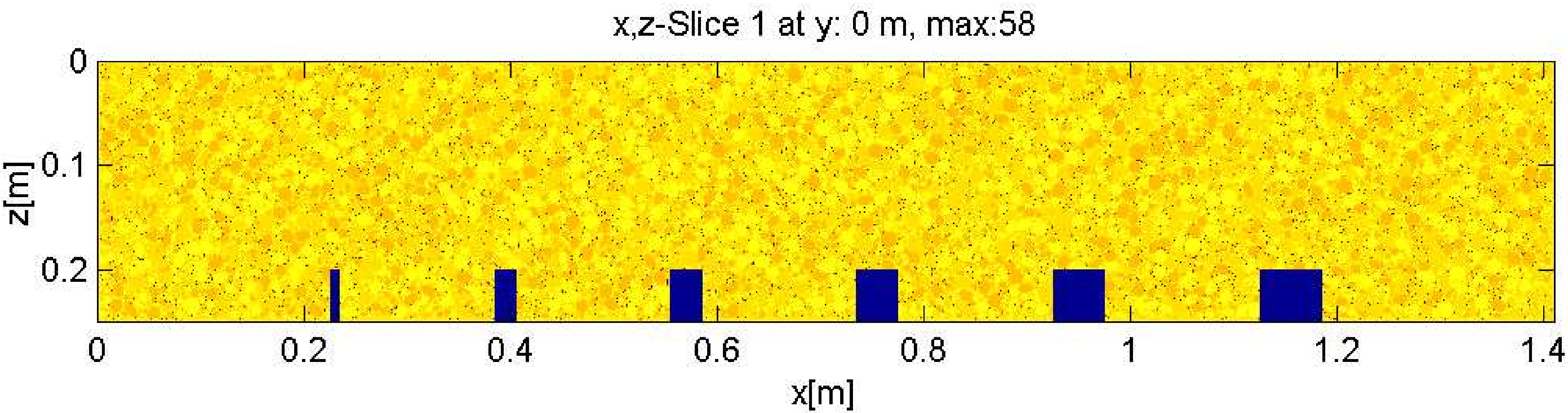

- data provided by K. Mayer, University of Kassel, Germany.
- simulation in homog. medium: $f_0 = 200$KHz, $c_0 = 4207$m/s
- experimental data: $f_0 = 150$KHz, $c_L = 4150$m/s
- Transmitter and receiver: Krautgrämer G0,2R

Real data: measurements

- Measurement acquisition geometry

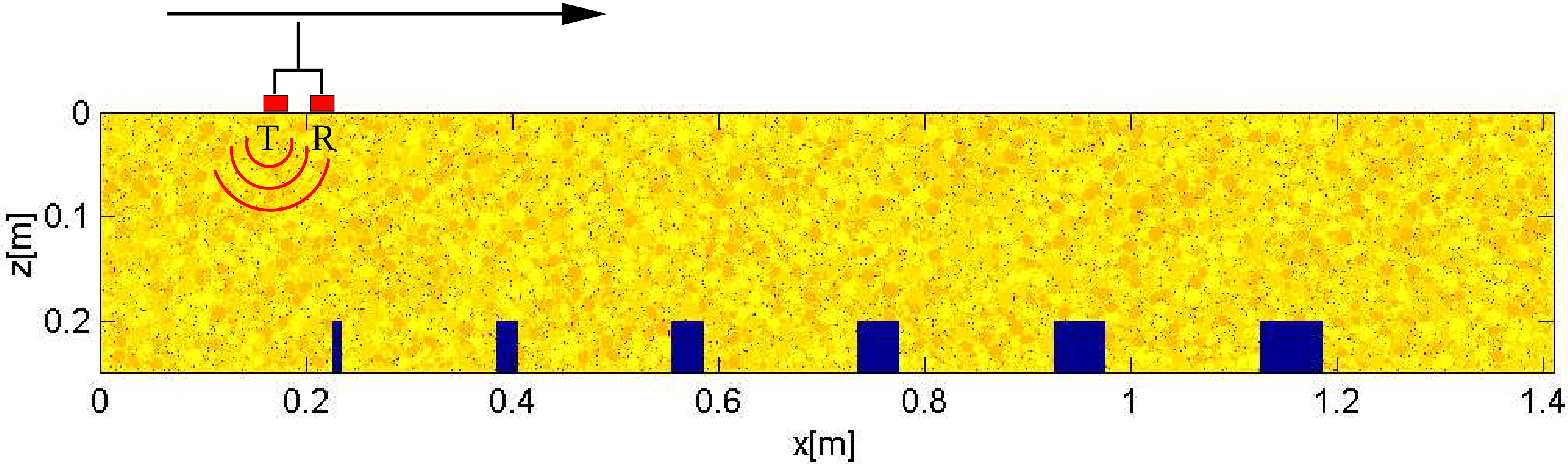

Real data: measurements

- Measurement acquisition geometry

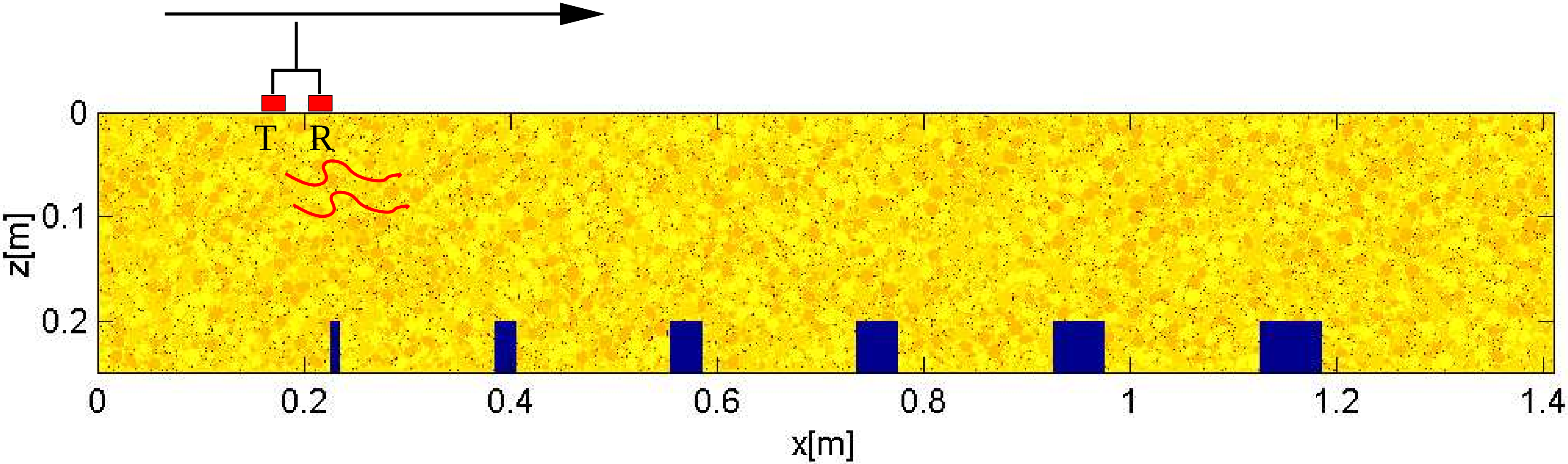

Real data: measurements

- Measurement acquisition geometry

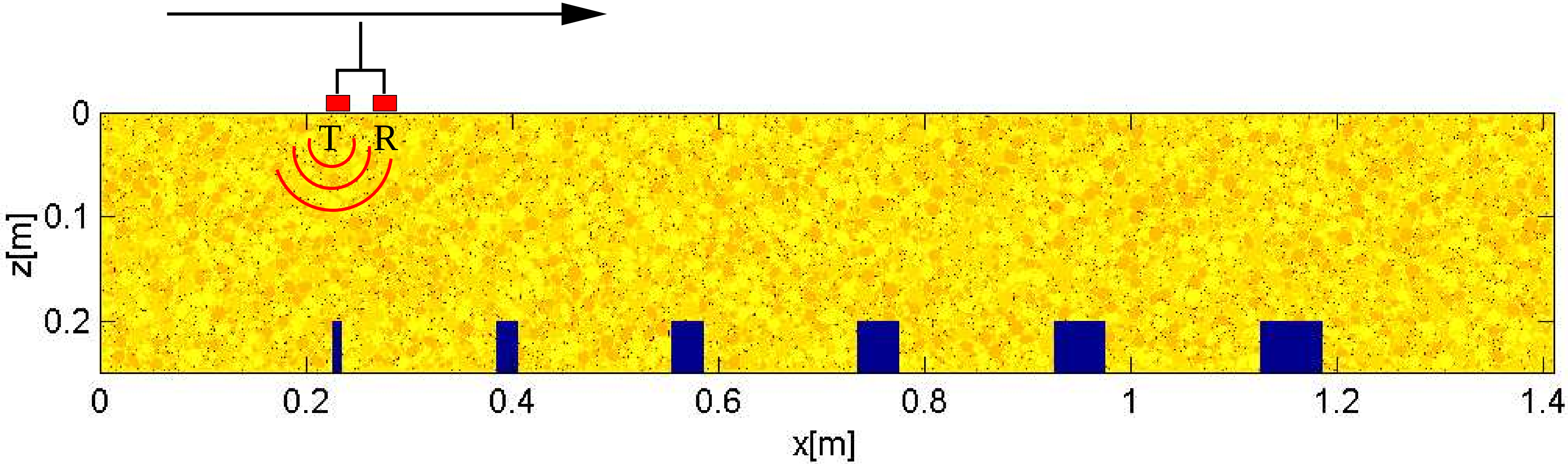

Real data: measurements

- Measurement acquisition geometry

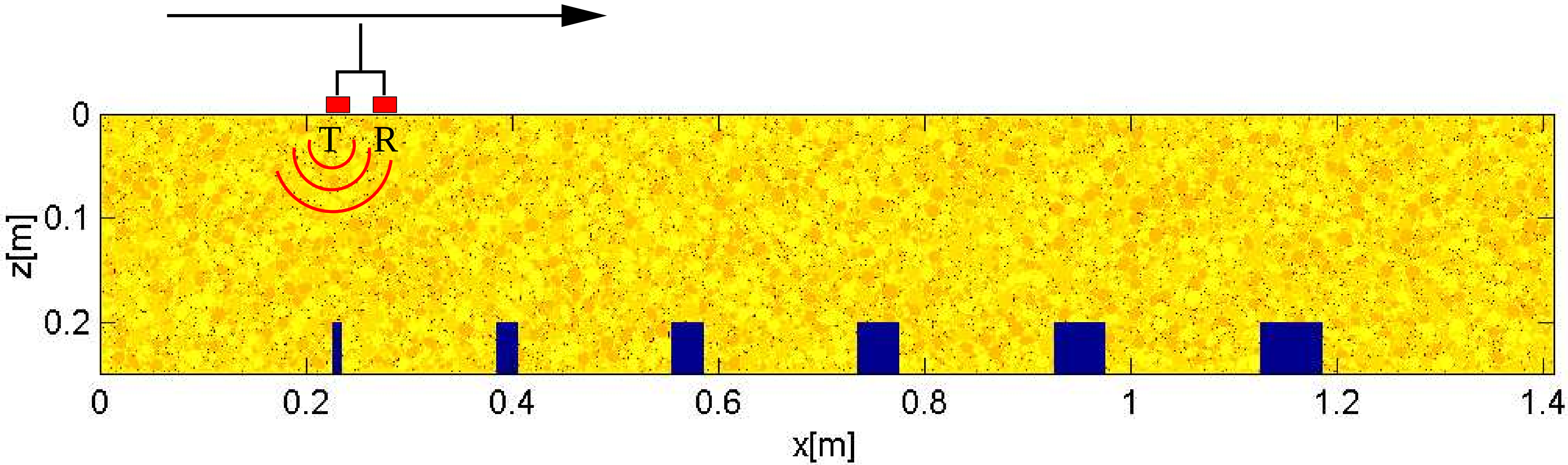

- Simulated data traces in homogeneous structure

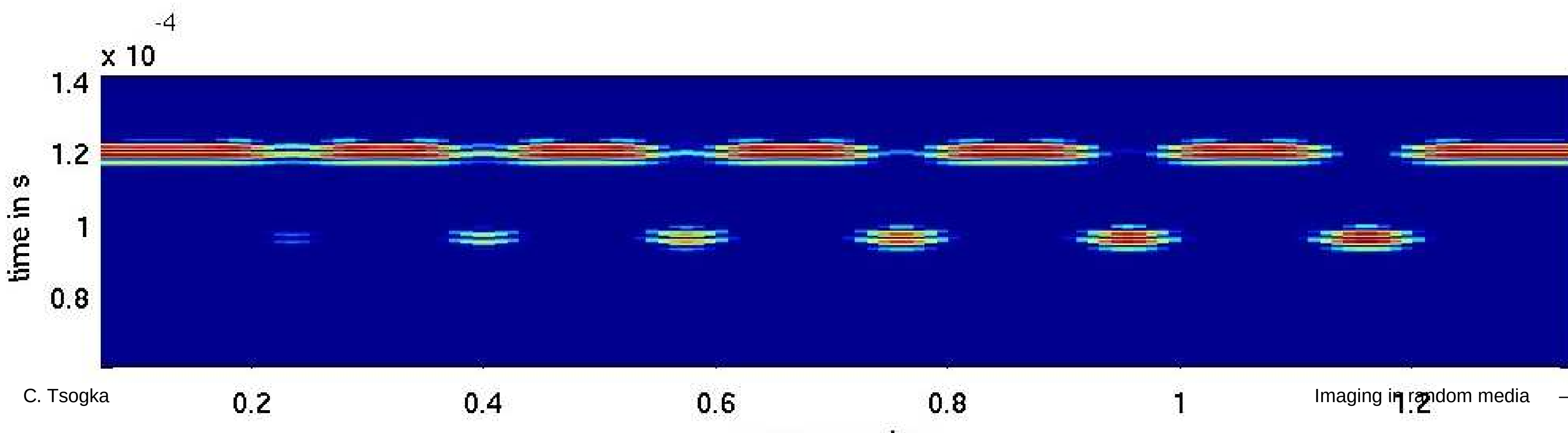

The CINT functional

- We rewrite the CINT imaging functional

$$\mathcal{I}^{\text{CINT}}(\mathbf{y}^S, \Omega_d, \kappa_d) = \int_B d\omega \int_{|\omega-\omega'|\leq\Omega_d} d\omega' \sum_{\mathbf{x}_m \in a} \sum_{|\mathbf{x}_m - \mathbf{x}_m{}'| \leq X_d(\omega)}$$

$$\hat{\mathcal{F}}(\mathbf{x}_m - \frac{d}{2}, \mathbf{x}_m + \frac{d}{2}, \omega, \mathbf{y}^s) \overline{\hat{\mathcal{F}}(\mathbf{x}_m{}' - \frac{d}{2}, \mathbf{x}_m{}' + \frac{d}{2}, \omega', \mathbf{y}^s)}$$

$$\hat{\mathcal{F}}(\mathbf{x}_s, \mathbf{x}_r, \omega, \mathbf{y}^S) = \hat{P}(\mathbf{x}_s, \mathbf{x}_r, \omega) e^{-i\omega\left(\tau(\mathbf{x}_s, \mathbf{y}^S) + \tau(\mathbf{x}_r, \mathbf{y}^S)\right)}$$

with

- $\mathbf{x}_m$: the midpoint moving on the array.
- d: distance between transmitter and receiver (fixed).
- $\mathbf{x}_s = \mathbf{x}_m - \dfrac{d}{2}$, $\mathbf{x}_r = \mathbf{x}_m + \dfrac{d}{2}$

Adaptive CINT results on real data

- Simulated data traces in homogeneous structure

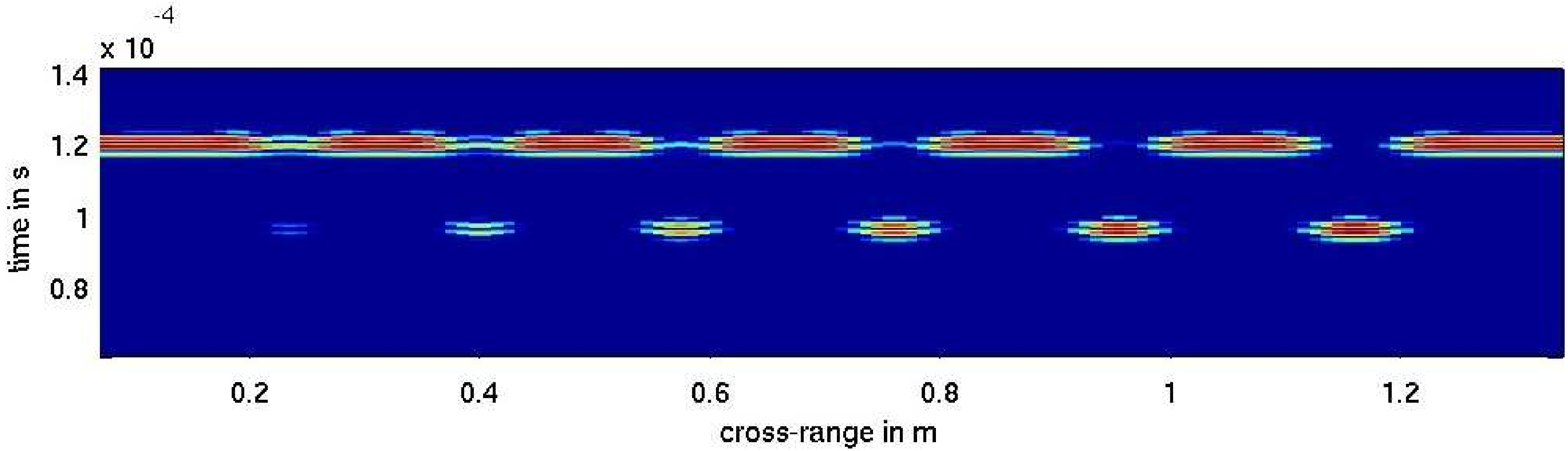

- Kirchhoff migration results

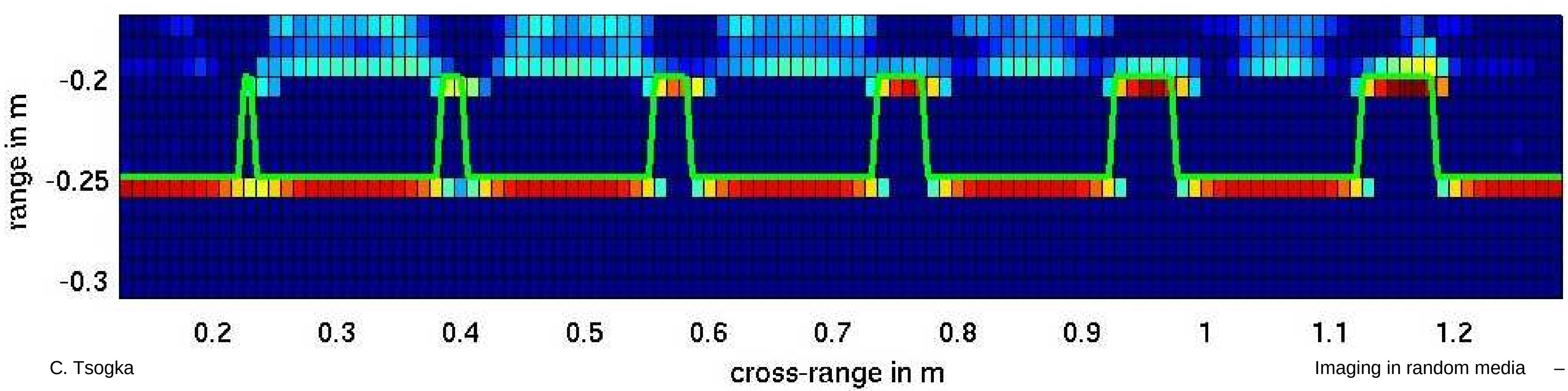

Adaptive CINT results on real data

- Data traces in the concrete structure

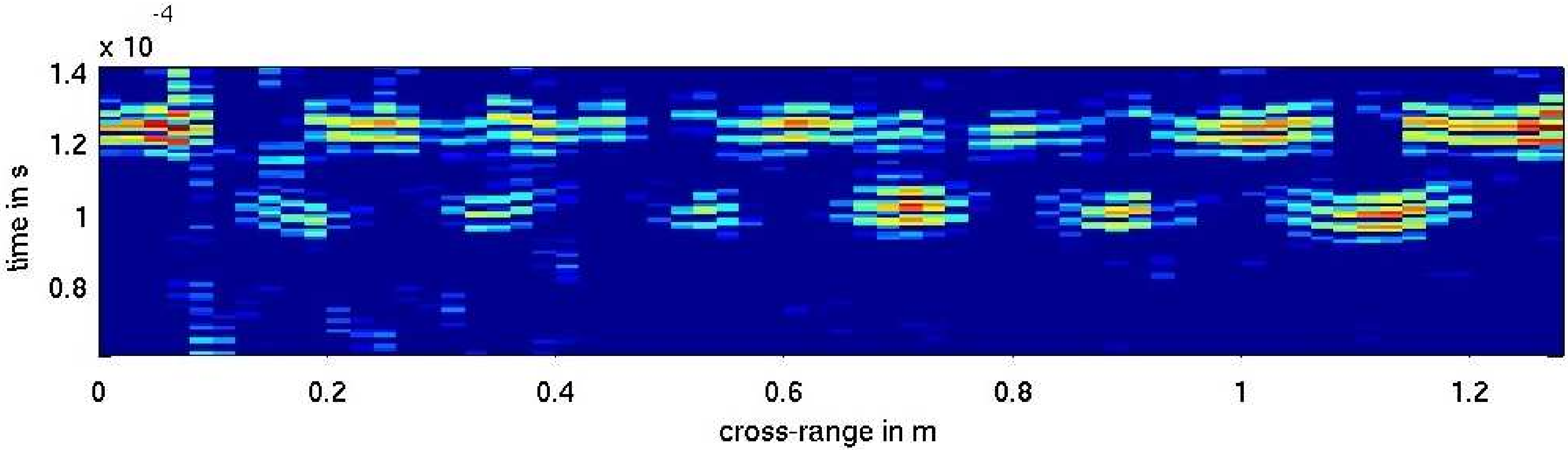

- Kirchhoff migration results

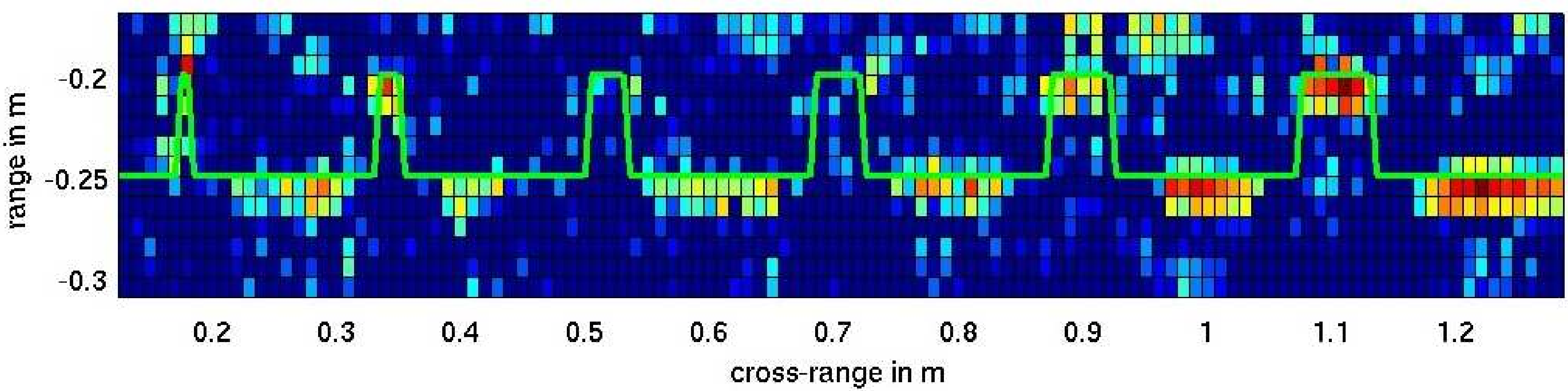

Adaptive CINT results on real data

- Adaptive CINT results

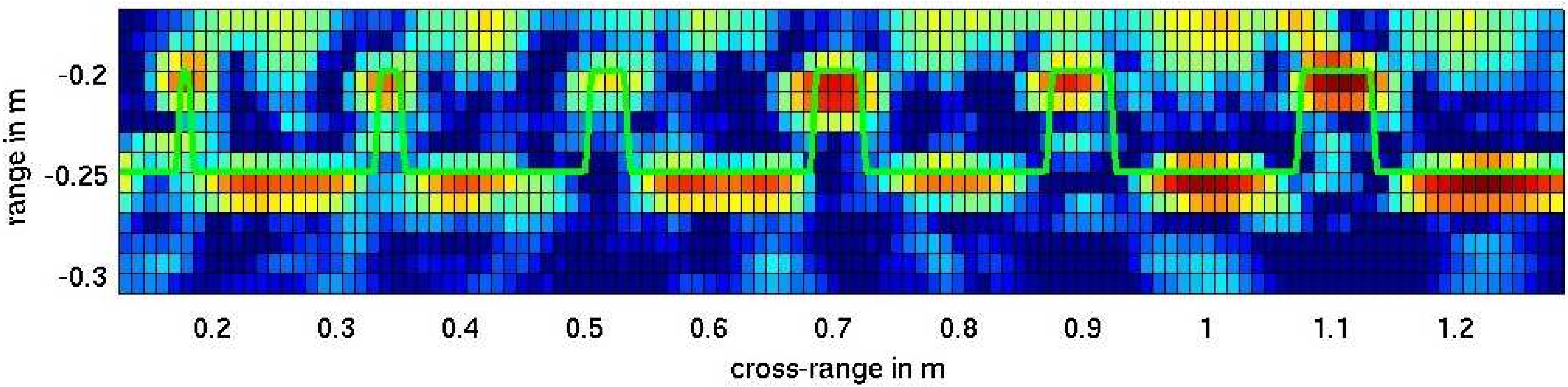

- Kirchhoff migration results